



## Nondiffusive hot spot in a confined, narrow domain

A.K. KAPILA<sup>1,\*</sup> and M. SHORT<sup>2</sup>

<sup>1</sup>*Department of Mathematical Sciences, Rensselaer Polytechnic Institute, Troy, NY 12180, U.S.A*

<sup>2</sup>*Department of Theoretical and Applied Mechanics, University of Illinois, 104 S. Wright Street, Urbana, IL 61801, U.S.A.*

Received 1 April 2002; accepted in revised form 10 December 2002

**Abstract.** The spatial structure and temporal evolution of a nondiffusive hot spot are examined in a confined, planar enclosure. The situation is modelled by the reactive Euler equations and single-step Arrhenius kinetics with a large (scaled) activation temperature  $1/\epsilon$ . The initial state of the medium is taken to be one of uniform pressure but with a prescribed thermal gradient of order  $\epsilon$  across the domain. The induction equations, which govern order  $\epsilon$  disturbances to the initial state, are analyzed in the limit of small  $\alpha$ , where  $\alpha$  measures the width of the domain relative to the acoustic length based on a characteristic reaction time at the initial state. The solution displays a sequence of finite-time singularities as the hot spot grows in strength and shrinks in size in a spatially homogeneous pressure environment. Ultimately, in a region of exponentially small size, significant pressure gradients appear as acoustic and reaction times become comparable and the hot-spot structure is found to obey the full, but previously analyzed, Clarke equations.

**Key words:** activation-energy asymptotics, Arrhenius kinetics, blowup, hot spot

### 1. Introduction

Explosive systems typically experience little chemical activity at room temperature and pressure. For an explosive event to occur, the system must be subjected to a thermal or mechanical stimulus that preconditions the sample, *i.e.*, raises its temperature to a level high enough to initiate chemical reaction. Such preconditioning can occur in a variety of ways, including subjecting the material to a shock, injecting a hot jet of combustion products into the unreacted material, and irradiating the medium with a burst of energy. While preconditioning may initiate a low level of chemical activity over a broad extent of the sample, a rapid acceleration of the rate of reaction usually occurs first at small, discrete sites where inherent nonuniformity in the state of the system causes the reaction to intensify preferentially and lead to localized explosions. Combustion waves originating from these reaction centers, or hot spots, eventually envelope the entire bulk.

A central problem in the theory of homogeneous reactive materials is a precise description of the manner in which a hot spot develops and grows in a given sample for a prescribed set of initial and boundary data. This growth may occur, locally, at nearly constant volume, at nearly constant pressure, or at conditions intermediate between these two extremes. To a considerable extent the structure of the hot spot determines the kind of combustion wave that will emerge from it, as well as the sequence of events that will occur prior to the establishment of a fully fledged wave. While the evolution is a function of the physico-chemical properties of the material, it also depends crucially on the size of the sample. In this paper we examine

---

\*kapila@rpi.edu

the problem in a planar, one-dimensional configuration wherein the material is confined to a narrow slot between two parallel, rigid boundaries, a geometry not uncommon in experimental setups. The material is taken to be a polytropic reacting fluid, undergoing an exothermic reaction governed by one-step Arrhenius kinetics with large activation temperature  $1/\epsilon$  in suitably scaled units. The initial state is taken to be weakly nonuniform, with the temperature decreasing monotonically from one wall to the other by an order  $\epsilon$  amount. The system is modelled by the reactive Euler equations, an appropriate description when the initial temperature is high enough so that the characteristic reaction time and acoustic travel time across the slot are much too short for diffusion to play a significant role in the evolutionary process. A unified formulation of diffusive and nondiffusive thermal explosion theory can be found in Kasoy, Kapila and Stewart [1].

Earlier studies have examined the situation in which the width of the slot is large enough so that the acoustic travel time between the boundaries is comparable to a characteristic reaction time at the initial state. For these wider regions, order  $\epsilon$  departures from the initial state, during the so-called induction period, are governed by the Clarke equations (see Clarke [2], Clarke and Cant [3] and Jackson and Kapila [4]), a small-disturbance description representing a balance between acoustics and weak but nonlinear chemical heat addition. Differential chemical heating of neighboring elements produces pressure waves that travel across the slot, thereby setting up significant pressure gradients. The induction period typically culminates in a localized thermal runaway at the hot boundary, characterized by singularities in pressure and temperature disturbances, while the density perturbation remains bounded. Thus a nearly-constant-volume explosion occurs at the runaway site, heralding the birth of a supersonic reaction wave that emerges from the hot spot, decelerates as it proceeds into the colder material, and eventually transitions into a ZND detonation. Here we are not concerned with these later events which have been studied extensively and comprehensively by asymptotic (Dold, Kapila and Short [5]) and numerical (Kapila, Schwendeman, Quirk and Hawa [6]) means, but with the structure of the induction singularity. A description of the asymptotically self-similar structure of the singularity was given by Jackson, Kapila and Stewart [7] for an initial temperature nonuniformity, and later by Parkins, Blythe and Crighton [8] in an elegant analysis that exploited the Newtonian limit of near-unity specific heats ratio ( $\gamma - 1 \ll 1$ ). Related problems in which the induction domain is contained between a piston and a shock (Blythe and Crighton [9]) or a contact surface and a shock (Parkins [10]) have also been similarly analyzed.

Our present concern is with narrower regions for which  $\alpha$ , the slot width referred to the acoustic length, is considerably smaller than unity;  $\alpha \ll 1$ . It is immediately clear that the system must now evolve differently during the induction stage, as acoustic waves can traverse the slot many times during a characteristic induction time, thereby ensuring that the pressure gradients are now much weaker than they were in the wider regions studied earlier. It is of interest then to determine how this difference in early evolution affects the subsequent events as far as the growth and structure of the hot spot are concerned.

The only analysis of this problem to date is that due to Kasoy, Riley, Bebernes and Bressan [11]. These authors examined the induction domain for the situation  $\alpha = \sqrt{\epsilon}$ , and found that the solution undergoes a nearly-constant-pressure thermal runaway. In this paper we show that their solution only tells part of the story, and that a further examination of the runaway singularity reveals a transition from a nearly-constant-pressure to a nearly-constant-volume behavior. We also show that with the exception of rather special initial conditions, the

induction solution exhibits a two time-scale structure, wherein a fast-time acoustic oscillation is superposed on a spatially-homogeneous pressure evolution.

The paper begins with a description of the model in Section 2. Section 3 introduces the small-disturbance induction equations, displays their numerical solution, and derives the asymptotic solution for the main induction stage in the limit  $\alpha \rightarrow 0$ . This solution exhibits a velocity singularity across the entire spatial domain, and a temperature singularity near the hot wall, at a finite runaway time  $t_c$ . In Section 4 the velocity singularity is resolved in a thin temporal layer, while Section 5 treats the temperature singularity in a thin corner region at the hot wall. Successive singularities of the solution in the shrinking corner are analyzed in Sections 6 and 7, and the paper culminates with a description of the by-now exponentially thin corner, in which the full Clarke equations are realized. The generic runaway behavior of these equations has a nearly-constant-volume, inertially confined structure. It has been examined in detail in [7], and provides the bridge to the post-induction phase of the local explosion.

## 2. The mathematical model

The state of the medium is specified by the pressure  $p'$ , density  $\rho'$  (or specific volume  $v' = 1/\rho'$ ), speed  $u'$  and temperature  $T'$ . Progress of reaction is measured by the mass fraction of the deficient reactant,  $Y'$ , which decreases in value from  $Y'_0$  to 0 as the reaction proceeds from initiation to completion. An unscaled quantity is signified by attaching a prime to the corresponding symbol, while absence of the prime indicates that the quantity has been scaled. The reference values for pressure, temperature and density are chosen to be the nominally uniform initial values  $p'_0$ ,  $T'_0$  and  $\rho'_0$ . With  $l'_0$  a reference length and  $t'_0$  a reference time, to be specified shortly, velocity is measured on the scale  $u'_0 = l'_0/t'_0$ . Pressure, temperature and density are related via the gas law

$$p' = \rho' \frac{R}{W} T',$$

where  $R$  is the universal gas constant and  $W$  the average molecular weight of the mixture, deemed to undergo little change during the reaction. The specific heats at constant volume and at constant pressure,  $C'_v$  and  $C'_p$  respectively, obey the relation

$$\frac{R}{W} = C'_p - C'_v.$$

For the simple one-step Arrhenius kinetics adopted here, the unit of time is selected to be

$$t'_0 = \frac{RT'_0}{\mathcal{E}'_a} \frac{1}{B'} \frac{C'_v T'_0}{Q'} \exp(\mathcal{E}'_a/RT'_0), \tag{2.1}$$

where  $B'$  is the pre-exponential frequency factor,  $\mathcal{E}'_a$  the activation energy and  $Q'$  the specific heat of reaction. It is convenient to employ a mass-weighted spatial variable  $x$ , defined in terms of the scaled spatial coordinate  $\xi$ , by

$$x = \int_0^\xi \rho(X, t) dX. \tag{2.1}$$

We now let  $x$  span the interval  $[0, 1]$  between the slot boundaries. The mass confined within the slot per unit cross-sectional area is then unity, and one is led to the constraint

$$1 = \int_0^{L'/l'_0} \rho(X, 0) dX$$

between the reference length  $l'_0$  and the slot width  $L'$ . Since we shall be concerned with near-unity initial densities, the above expression implies that the two lengths are nearly identical.

The initial temperature is assumed to be high enough to make the characteristic chemical times short compared to the times associated with diffusive transport, so that diffusion can be ignored. Then the governing equations are simply those of reactive gasdynamics, written below in the dimensionless form,

$$\alpha^2 u_t + \frac{1}{\gamma} p_x = 0, \quad (2.3)$$

$$p u_x + \frac{1}{\gamma} v p_t = W, \quad (2.4)$$

$$T_t - \frac{\gamma - 1}{\gamma} v p_t = W, \quad (2.5)$$

along with the equation for reactant consumption,

$$Y_t = -\frac{1}{\beta} W, \quad (2.6)$$

the gas law,

$$T = p v, \quad (2.7)$$

and the reaction rate,

$$W = \epsilon Y \exp \left[ \frac{1}{\epsilon} \left( 1 - \frac{1}{T} \right) \right]. \quad (2.8)$$

The parameters appearing above are the specific heats ratio  $\gamma = C'_p/C'_v$ , the scaled inverse activation energy  $\epsilon = RT'_0/\mathcal{E}'_a$ , the scaled heat of reaction  $\equiv Q'/C'_v T'_0$ , and the scaled slot width  $\alpha = l'_0/l'_a$ , where  $l'_a$  is a characteristic acoustic length. It is defined as  $l'_a = t'_0 c'_0$ , where  $c'_0 = \sqrt{\gamma p'_0/\rho'_0}$  is the acoustic speed at the reference state. The analysis will proceed under the assumptions that the dimensionless activation energy is large and the scaled slot width small, with the corresponding dimensionless parameters ordered as

$$\epsilon \ll \alpha^2 \ll 1. \quad (2.9)$$

We now turn to the boundary and initial conditions. The confining walls are rigid, so that

$$u(0, t) = u(1, t) = 0. \quad (2.10)$$

The initial distributions of pressure and reactant mass fraction are taken to be uniform, while a weak initial velocity field is admitted. Therefore,

$$p(x, 0) = Y(x, 0) = 1, \quad u(x, 0) = \epsilon U_i(x). \quad (2.11)$$

It is assumed that the spatially nonuniform ignition process is driven by an  $O(\epsilon)$  initial thermal variation across the slot, given by

$$T(x, 0) = 1 + \epsilon T_i(x). \tag{2.12}$$

We have in mind a monotonic initial temperature profile, with the hottest point at the left wall. Following [8] the specific form

$$T_i(x) = -\log(1 + ax), \quad a > 0, \tag{2.13}$$

is chosen simply for analytical tractability. We postpone the specification of  $U_i$  until the following section.

### 3. Induction

Consistent with the initial data, we anticipate an induction phase during which the state of the medium will undergo an  $O(\epsilon)$  variation. Thus we seek the asymptotic expansions

$$p(x, t, \alpha, \epsilon) \sim 1 + \epsilon \gamma P(x, t, \alpha) + \dots, \tag{3.1}$$

$$T(x, t, \alpha, \epsilon) \sim 1 + \epsilon \mathcal{T}(x, t, \alpha) + \dots, \tag{3.2}$$

$$v(x, t, \alpha, \epsilon) \sim 1 + \epsilon V(x, t, \alpha) + \dots, \tag{3.3}$$

$$u(x, t, \alpha, \epsilon) \sim 0 + \epsilon U(x, t, \alpha) + \dots, \tag{3.4}$$

$$Y(x, t, \alpha, \epsilon) \sim 1 - \frac{\epsilon}{\beta} Z(x, t, \alpha) + \dots. \tag{3.5}$$

Substitution into (2.3) – (2.8) leads to the induction equations

$$\alpha^2 \frac{\partial U}{\partial t} + \frac{\partial P}{\partial x} = 0, \tag{3.6}$$

$$\frac{\partial P}{\partial t} + \frac{\partial U}{\partial x} = e^{\mathcal{T}}, \tag{3.7}$$

$$\frac{\partial \mathcal{T}}{\partial t} - (\gamma - 1) \frac{\partial P}{\partial t} = e^{\mathcal{T}}, \tag{3.8}$$

$$V = \mathcal{T} - \gamma P, \tag{3.9}$$

$$\frac{\partial Z}{\partial t} = e^{\mathcal{T}}. \tag{3.10}$$

First derived by Clarke [2], these equations reflect a balance between linearized acoustics and weak but nonlinear exothermicity. The first three equations of this set suffice to determine  $P$ ,  $\mathcal{T}$  and  $U$ , and then the remaining two readily yield  $V$  and  $Z$ . In fact, on combining (3.8) and (3.10) and integrating, we obtain

$$Z = \mathcal{T} - (\gamma - 1)P + \log(1 + ax). \tag{3.11}$$

It is also instructive to eliminate  $P$  and  $U$  in favor of  $\mathcal{T}$  from Equations (3.6–3.8). The result is the third-order wave equation

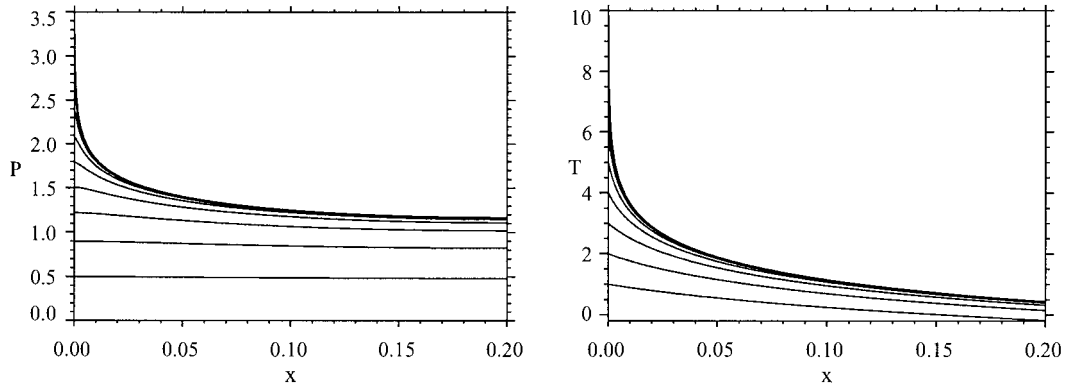


Figure 1.  $P$  and  $\mathcal{T}$  profiles for  $\gamma = 1.4$ ,  $a = 1$  and  $\alpha = 0.2$ . The profiles are shown at times 0.50398, 0.69855, 0.77289, 0.80072, 0.81101, 0.81478, 0.81615, 0.81666, 0.81684 and 0.81691. Two features are worth noting: the spatial uniformity of the pressure at times prior to runaway, and the slow rise in the hot-wall pressure, compared to temperature, as runaway is approached.

$$\left(\frac{\partial^2}{\partial x^2} - \alpha^2 \frac{\partial^2}{\partial t^2}\right) \frac{\partial \mathcal{T}}{\partial t} = \left(\frac{\partial^2}{\partial x^2} - \gamma \alpha^2 \frac{\partial^2}{\partial t^2}\right) e^{\mathcal{T}},$$

containing elementary wave operators with associated speeds  $1/\alpha$  and  $1/\alpha\sqrt{\gamma}$ .

For  $\alpha = 1$  the induction equations have been extensively studied ([2–4], [8–10]). The onset of ignition is signalled by the appearance of a finite-time blowup in the induction solution. The blowup is characterized by  $\mathcal{T}$  and  $P$  becoming logarithmically singular while  $V$  remains finite. The spatial structure of the singularity was analyzed by Jackson, Kapila and Stewart [7]. Their study also took the analysis beyond the induction regime and considered the full reactive Euler equations, thereby elucidating the exponentially rapid development of the local explosion as well as the effect of reactant depletion.

Here we are concerned with  $\alpha \ll 1$ . Further analysis in this limit is facilitated by setting

$$\mathcal{T} = -\log \psi, \tag{3.12}$$

whereby (3.7) and (3.8) acquire the alternate forms

$$\frac{\partial U}{\partial x} + \frac{\partial P}{\partial t} = \frac{1}{\psi}, \tag{3.13}$$

$$\frac{\partial \psi}{\partial t} + (\gamma - 1) \frac{\partial P}{\partial t} \psi = -1, \tag{3.14}$$

which can be combined into

$$\frac{1}{\psi} \frac{\partial \psi}{\partial t} + \gamma \frac{\partial P}{\partial t} + \frac{\partial U}{\partial x} = 0. \tag{3.15}$$

In view of (2.11) and (2.13), the initial conditions are

$$P(x, 0) = 0, \quad U(x, 0) = U_i(x), \quad \psi(x, 0) = 1 + ax. \tag{3.16}$$

Figure 1 above shows the results of a numerical computation of the equation set (3.6)–(3.8). The important difference from the  $\alpha = O(1)$  case lies in the acoustic time across the

vessel being short, thereby allowing an acoustic disturbance to traverse the slot many times over a characteristic chemical time and equilibrate the pressure. Equation (3.6) implies that to  $O(\alpha^2)$ ,  $P = P(t)$ . Upon an integration across the slot, (3.15) yields

$$P'(t) = -\frac{1}{\gamma} \int_0^1 \frac{1}{\psi} \frac{\partial \psi}{\partial t} dx, \tag{3.17}$$

where we have applied the rigid-wall boundary conditions (2.10). A further integration in  $t$  and the use of the initial conditions (3.16a,c) leads to

$$P = -\frac{1}{\gamma} \int_0^1 [\log \psi - \log(1 + ax)] dx. \tag{3.18}$$

Equation (3.14), being linear in  $\psi$ , can also be integrated with respect to  $t$  to yield

$$\begin{aligned} \psi &= e^{-(\gamma-1)P(t)} \left[ 1 + ax - \int_0^t e^{(\gamma-1)P(\lambda)} d\lambda \right] \\ &= e^{-(\gamma-1)P(t)} [r(t) + ax], \end{aligned} \tag{3.19}$$

where

$$r(t) \equiv 1 - \int_0^t e^{(\gamma-1)P(\lambda)} d\lambda. \tag{3.20}$$

We now have two expressions, (3.18) and (3.19), relating  $P$  and  $\psi$ . Elimination of  $\psi$  between the pair leads to the integral equation,

$$\begin{aligned} P(t) &= -\int_0^1 \left[ \ln \left\{ 1 + ax - \int_0^t e^{(\gamma-1)P(\lambda)} d\lambda \right\} - \log(1 + ax) \right] dx, \\ &= -\int_0^1 [\log\{r(t) + ax\} - \log\{1 + ax\}] dx \\ &= -\frac{1}{a} [r(t) + a] \log\{r(t) + a\} - r(t) \log r(t) - (1 + a) \log(1 + a), \end{aligned} \tag{3.21}$$

whose solution provides  $P$  implicitly. Then (3.19) determines  $\psi$ , and following an integration with respect to  $x$ , (3.13) yields  $U$ ,

$$\begin{aligned} U &= -P'(t)x + \int_0^x \frac{1}{\psi} dx \\ &= -P'(t)x + \frac{1}{a} e^{(\gamma-1)P(t)} \log \frac{r(t) + ax}{r(t)}. \end{aligned} \tag{3.22}$$

Several observations are now in order.

First, the integral Equation (3.21) for  $P$ , in conjunction with the definition (3.20) of  $r(t)$ , can be converted into the following differential equation for  $r$  :

$$\frac{dr}{dt} = -\exp \left\{ -\frac{\gamma-1}{a} [r+a] \log\{r+a\} - r \log r - (1+a) \log(1+a) \right\}, \quad r(0) = 1. \tag{3.23}$$

From the solution  $r(t)$ ,  $P$  can in principle be determined by the relation

$$P(t) = \frac{1}{\gamma-1} \log \left( -\frac{dr}{dt} \right). \tag{3.24}$$

Second, the solution has a limited range of validity; (3.19) shows that  $\psi$  vanishes at  $x = 0$  at a critical time  $t_c$  given by

$$\int_0^{t_c} e^{(\gamma-1)P(\lambda)} d\lambda = 1, \quad (3.25)$$

or equivalently, by  $r(t_c) = 0$ , thereby leading to the explicit expression

$$t_c = \int_0^1 \exp \left\{ \frac{\gamma-1}{a} [r+a] \log[r+a] - r \log r - (1+a) \log(1+a) \right\} dr. \quad (3.26)$$

Thus there appears a local logarithmic singularity in  $\mathcal{T}$  indicative of a thermal runaway, or blowup, at the hot wall. At the same time (3.21) shows that  $P(t_c)$ , given by

$$P(t_c) \equiv -\frac{1}{a} [a \log a - (1+a) \log(1+a)], \quad (3.27)$$

is bounded, while (3.22) shows  $U$  to be logarithmically singular at  $t = t_c$  throughout the interior of the slot. Thus the blowup singularity now has a markedly different character than the inertially confined, nearly-constant-volume structure described by Jackson, Kapila and Stewart [7] for  $\alpha$  of order unity.

Third, the expression (3.22) above for  $U(x, t)$  has the initial value

$$\begin{aligned} U(x, 0) &= -P'(0)x + \frac{1}{a} e^{(\gamma-1)P(0)} \log \frac{r(0) + ax}{r(0)} \\ &= \frac{1}{a} [-x \log(1+a) + \log(1+ax)]. \end{aligned} \quad (3.28)$$

As a result, the solution derived above holds only if the initial condition  $U_i(x)$  is chosen to be in accord with this initial value. Otherwise one must introduce an initial layer in which the solution is found to exhibit a high-frequency oscillation with time scale  $t/\alpha$ , which intrudes into the main induction region and modifies the solution therein. In fact, the solution in the main induction region must then contain both the fast and the slow time scales,  $t$  and  $t/\alpha$ . We have carried out such an analysis; it is algebraically more complex than the treatment given here, but shows that the inclusion of the high-frequency component in the induction solution does not alter the nature of the runaway singularity. For ease of presentation, therefore, we adopt the special initial condition on  $U$  as required by (3.28) above. A brief discussion of the initial layer for general  $U_i(x)$  is given in Appendix A1.

In their treatment of the induction zone, Kassoy *et al.* [11] arrived at expressions for  $P$  and  $\mathcal{T}$  equivalent to those derived above, albeit for a general initial temperature distribution and for an arbitrary number of space dimensions. They did not, however, appear to recognize the appearance of the fast-time behavior for an arbitrary initial distribution of  $U$ , nor did they proceed beyond the first appearance of runaway.

### 3.1. NEAR-BLOWUP BEHAVIOR

In order to delve further into the structure of the singularity we need to examine the asymptotic nature of the induction solution at blowup, both within the slot,  $0 < x < 1$ , and near the hot wall,  $x \approx 0$ . Since  $P(t)$  has been expressed above in terms of  $r$ , and both  $\psi$  and  $U$  in terms of  $r$  and  $P$ , it is convenient to begin by seeking an expansion for  $r$  as  $s \equiv t_c - t \rightarrow 0$ . We recognize that in view of (3.25),  $r(t)$ , defined in (3.20), can be re-expressed as



$$r(t) = \int_0^{t_c} e^{(\gamma-1)P(\lambda)} d\lambda - \int_0^t e^{(\gamma-1)P(\lambda)} d\lambda = \int_t^{t_c} e^{(\gamma-1)P(\lambda)} d\lambda. \quad (3.29)$$

Thus  $r(t)$  vanishes at blowup and therefore can be viewed as a distorted time to runaway. The leading term in the small  $s$  expansion of  $r$  is readily available from (3.29) as

$$r(t) \sim (t_c - t)e^{(\gamma-1)P(t_c)} + \dots = cs + \dots, \quad (3.30)$$

where

$$c \equiv e^{(\gamma-1)P(t_c)}. \quad (3.31)$$

Computation of higher-order terms in (3.30) requires knowledge of the behavior of  $P$  to orders beyond the leading term  $P(t_c)$ . To that end we turn to (3.21) and expand for small  $r$  to get

$$\begin{aligned} P(t) &\sim -\frac{1}{a} \left[ a \log a - (1+a) \log(1+a) \right] - \frac{1}{a} \left[ -r \log r + (1 + \log a)r + \frac{r^2}{2a} + \dots \right] \\ &= P(t_c) - \frac{1}{a} \left[ -r \log r + (1 + \log a)r + \frac{r^2}{2a} + \dots \right]. \end{aligned} \quad (3.32)$$

Replacement of  $r$  by its just-derived asymptotic form  $cs$  leads to the desired asymptotic expansion of  $P$ ,

$$P \sim P(t_c) + \frac{cs}{a} \log \frac{cs}{a} - \frac{cs}{a} + \dots, \text{ as } s \rightarrow 0. \quad (3.33)$$

Since  $P$  is a function of  $t$  alone the above result holds throughout the slot. When substituted in (3.29) the above expression leads, in turn, to the higher-order asymptotic form of  $r$ ,

$$r \sim a \left[ \frac{cs}{a} + \frac{\gamma-1}{2} \left\{ \frac{c^2 s^2}{a^2} \log \frac{cs}{a} - \frac{3}{2} \frac{c^2 s^2}{a^2} + \dots \right\} \right], \quad (3.34)$$

which will be of use in the sequel.

In order to determine the behavior of  $\psi$  for  $s \rightarrow 0$  we turn to (3.19) and substitute in it the above expansions for  $r$  and  $P$ . The results depend upon whether  $s \rightarrow 0$  with  $x > 0$  and fixed (slot interior) or  $x/s$  fixed (near hot wall), and are gathered below.

$$\psi \sim \begin{cases} \frac{a}{c} \left[ x + \frac{cs}{a} \left\{ 1 - (\gamma-1)x \left( \log \frac{cs}{a} - 1 \right) \right\} + \dots \right] & \text{for } x = O(1), s \rightarrow 0; \\ \frac{a}{c} \left[ x + \frac{cs}{a} + (\gamma-1) \frac{cs}{a} \left\{ -\frac{1}{2} \frac{cs}{a} \log \frac{cs}{a} + \frac{1}{4} \frac{cs}{a} - x \log \frac{cs}{a} + x \right\} + \dots \right] & \text{for } x/s = O(1), s \rightarrow 0. \end{cases} \quad (3.35)$$

Figure 2 shows the numerically obtained near-blowup behavior of  $\psi(0, t)$ . From the graph the blowup time can be estimated to be  $t_c(\text{numerical}) = 0.81712$ . This is closely matched by the leading-order asymptotic value of 0.82709, given by (3.26).

Finally we turn to the expression (3.22) for  $U$ . It requires, first, an expansion for  $dP/dt$  which is obtained from (3.32) with the aid of (3.34) as

$$\frac{dP}{dt} \sim \frac{c}{a} \left[ -\log \frac{cs}{a} + \left\{ (\gamma-1) \left( -\frac{cs}{a} \log^2 \frac{cs}{a} + \frac{1}{2} \frac{cs}{a} \log \frac{cs}{a} + \frac{3}{4} \frac{cs}{a} \right) + \frac{cs}{a} \right\} + \dots \right], \text{ as } s \rightarrow 0. \quad (3.36)$$

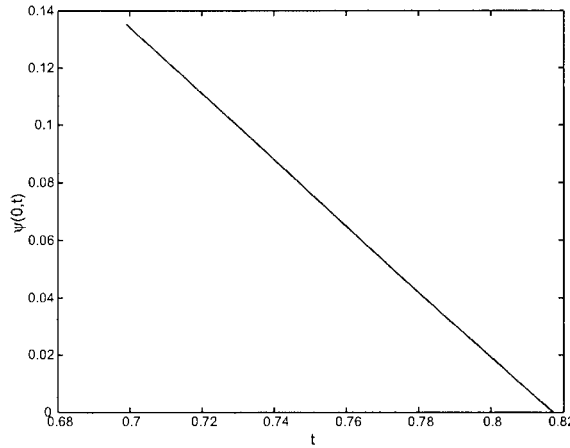


Figure 2. Numerically-computed near-blowup graph of  $\psi(0, t)$  for  $\gamma = 1.4$ ,  $a = 1$  and  $\alpha = 0.2$ .

Second, upon using (3.33), we obtain

$$e^{(\gamma-1)P(t)} \sim c \left[ 1 + (\gamma - 1) \left( \frac{cs}{a} \log \frac{cs}{a} - \frac{cs}{a} \right) + \dots \right]. \tag{3.37}$$

Third, we expand  $\log[(r + ax)/r]$  to get

$$\log\left(\frac{r + ax}{r}\right) \sim \begin{cases} -\log \frac{cs}{a} + \log x - \frac{\gamma - 1}{2} \left( \frac{cs}{a} \log \frac{cs}{a} - \frac{3cs}{2a} \right) + \frac{cs}{ax} & \text{for } x = O(1), s \rightarrow 0; \\ \log\left(1 + \frac{ax}{cs}\right) - \frac{\gamma - 1}{2} \frac{\{\log(cs/a) - 3/2\}x}{1 + ax/cs} & \text{for } x/s = O(1), s \rightarrow 0. \end{cases} \tag{3.38}$$

The last three results may now be substituted in (3.22) to yield

$$U \sim \frac{c}{a} \left[ -(1-x) \log \frac{cs}{a} + \log x - \left(x - \frac{1}{x}\right) \frac{cs}{a} + (\gamma - 1) \frac{cs}{a} \left\{ (x-1) \left( \log^2 \frac{cs}{a} - \frac{1}{2} \log \frac{cs}{a} - \frac{3}{4} \right) + \log x \left( \log \frac{cs}{a} - 1 \right) \right\} \right] + \dots \text{ for } x = O(1), s \rightarrow 0, \tag{3.39}$$

and

$$U \sim \frac{c}{a} \left[ \log\left(1 + \frac{ax}{cs}\right) + x \log \frac{cs}{a} - \frac{\gamma - 1}{2} \frac{\{\log(cs/a) - 3/2\}x}{1 + ax/cs} + (\gamma - 1) \frac{cs}{a} \left( \log \frac{cs}{a} - 1 \right) \log\left(1 + \frac{ax}{cs}\right) \right] + \dots \text{ for } x/s = O(1), s \rightarrow 0. \tag{3.40}$$

With the blowup behavior established, *i.e.*,  $P$  bounded,  $U$  logarithmically singular in the interior and  $\mathcal{T} = -\log \psi$  exhibiting a similar singularity at the hot wall, further evolution requires separate consideration of a thin interior layer and a corner region at the hot wall.

#### 4. Interior slotwide layer

The temporally thin layer in the interior of the slot is provoked by the singularity in  $U$  and characterized by  $x > 0$  and fixed, and  $s = \alpha\tau$ . The blowup behavior found above in (3.32), (3.35 a) and (3.39) provides the following matching conditions for the layer as  $\tau \rightarrow \infty$  :

$$P \sim P(t_c) + \alpha \left( \frac{c\tau}{a} \log \alpha + \frac{c\tau}{a} \log \frac{c\tau}{a} - \frac{c\tau}{a} \right), \quad (4.1)$$

$$\psi \sim \frac{a}{c} \left[ x - (\gamma - 1)\alpha x \left( \frac{c\tau}{a} \log \alpha + \frac{c\tau}{a} \log \frac{c\tau}{a} - \frac{c\tau}{a} \right) + \alpha \frac{c\tau}{a} \right], \quad (4.2)$$

$$U \sim \frac{c}{a} \left[ -(1-x) \log \alpha - (1-x) \log \frac{c\tau}{a} + \log x \right]. \quad (4.3)$$

The governing equations, obtained by transforming the induction set (3.6), (3.13) and (3.14) to the layer coordinates, are

$$-\alpha \frac{\partial U}{\partial \tau} + \frac{\partial P}{\partial x} = 0, \quad (4.4)$$

$$-\frac{\partial P}{\partial \tau} + \alpha \frac{\partial U}{\partial x} = \frac{\alpha}{\psi}, \quad (4.5)$$

$$\frac{\partial \psi}{\partial \tau} + (\gamma - 1)\psi \frac{\partial P}{\partial \tau} = \alpha. \quad (4.6)$$

We note from Equation (4.4) that in contrast to the induction solution wherein pressure was spatially homogeneous with an  $O(\alpha^2)$  error, pressure gradients in the layer are now of order  $\alpha$ . Guided by the matching conditions we seek the expansions

$$P \sim P(t_c) + \alpha \frac{c\tau}{a} \log \alpha + \alpha \tilde{P}, \quad (4.7)$$

$$\psi \sim \frac{ax}{c} - (\gamma - 1)\alpha \log \alpha x\tau + \alpha \tilde{\psi}, \quad (4.8)$$

$$U \sim -\log \alpha \frac{c}{a}(1-x) + \tilde{U}. \quad (4.9)$$

At  $O(\alpha \log \alpha)$  the energy equation (4.6) is satisfied identically. At  $O(\alpha)$  it reduces to

$$\frac{\partial \tilde{\psi}}{\partial \tau} + (\gamma - 1) \frac{ax}{c} \frac{\partial \tilde{P}}{\partial \tau} = 1,$$

which integrates to yield

$$\tilde{\psi} = \tau - (\gamma - 1) \frac{ax}{c} \tilde{P}. \quad (4.10)$$

Matching with (4.2) shows the function of integration to be zero. The momentum and mass equations (4.4) and (4.5) reduce to

$$\tilde{P}_x - \tilde{U}_\tau = 0,$$

$$\tilde{U}_x - \tilde{P}_\tau = \frac{c}{ax},$$

or, in characteristic form, to

$$(\tilde{P} + \tilde{U})_x - (\tilde{P} + \tilde{U})_\tau = \frac{c}{ax}, \quad (4.11)$$

$$(\tilde{P} - \tilde{U})_x + (\tilde{P} - \tilde{U})_\tau = -\frac{c}{ax}. \quad (4.12)$$

These equations have the general solution

$$\tilde{P} - \tilde{U} = -\frac{c}{a} \log x - 2f_1(\tau - x), \quad (4.13)$$

$$\tilde{P} + \tilde{U} = \frac{c}{a} \log x + 2g_1(\tau + x), \quad (4.14)$$

whence

$$\tilde{P} = -f_1(\tau - x) + g_1(\tau + x), \quad (4.15)$$

$$\tilde{U} = \frac{c}{a} \log x + f_1(\tau - x) + g_1(\tau + x), \quad (4.16)$$

where the functions  $f_1$  and  $g_1$  are to be determined. The far-wall condition

$$\tilde{U}(1, \tau) = 0 \quad (4.17)$$

provides the relation

$$f_1(\tau - 1) + g_1(\tau + 1) = 0,$$

which can also be written as

$$f_1(\tau - 2) + g_1(\tau) = 0. \quad (4.18)$$

As  $x \rightarrow 0$  we anticipate (see analysis in the following section) that the corner region at the wall will provide the matching condition

$$f_1(\tau) + g_1(\tau) = -\frac{c}{a} \log \frac{c\tau}{a}. \quad (4.19)$$

Elimination of  $g_1$  from the last two equations leads to a difference equation for  $f_1$ ,

$$f_1(\tau) - f_1(\tau - 2) = -\frac{c}{a} \log \frac{c\tau}{a}. \quad (4.20)$$

To obtain the initial condition for this difference equation we appeal to (4.1) and (4.3), the matching conditions for  $\tilde{P}$  and  $\tilde{U}$ , respectively. These provide the asymptotic expressions

$$\tilde{U} \sim \frac{c}{a} \log x - (1 - x) \frac{c}{a} \log \frac{c\tau}{a}, \quad (4.21)$$

$$\tilde{P} \sim \frac{c\tau}{a} \log \frac{c\tau}{a} - \frac{c\tau}{a}, \quad (4.22)$$

which, when applied to (4.13), yield

$$-2f_1(\tau - x) \sim \frac{c\tau}{a} \log \frac{c\tau}{a} - \frac{c\tau}{a} + \frac{c}{a}(1-x) \log \frac{c\tau}{a}, \text{ as } \tau \rightarrow \infty. \quad (4.23)$$

This result, in view of the asymptotic relations

$$\log \frac{c(\tau - x)}{a} \sim \log \frac{c\tau}{a} - \frac{x}{\tau},$$

and

$$\frac{c(\tau - x)}{a} \log \frac{c\tau}{a} \sim \frac{c(\tau - x)}{a} \log \frac{c(\tau - x)}{a} + \frac{cx}{a},$$

can be rearranged into the form

$$-2f_1(\tau - x) \sim \frac{c(\tau - x)}{a} \log \frac{c(\tau - x)}{a} - \frac{c(\tau - x)}{a} + \frac{c}{a} \log \frac{c(\tau - x)}{a},$$

or equivalently, as

$$f_1(\tau) \sim -\frac{c\tau}{2a} \log \frac{c\tau}{a} + \frac{c\tau}{2a} - \frac{c}{2a} \log \frac{c\tau}{a}, \text{ as } \tau \rightarrow \infty. \quad (4.24)$$

The solution to the difference equation (4.20) can now be found by inspection as

$$f_1(\tau) = \frac{c}{2a} \log(2\pi) - \frac{c(\tau + 1)}{2a} \log \frac{2c}{a} - \frac{c}{a} \log \left[ \Gamma \left( 1 + \frac{\tau}{2} \right) \right], \quad (4.25)$$

where  $\Gamma$  denotes the gamma function. Then, equation (4.18) determines  $g_1(\tau)$  as

$$g_1(\tau) = -f_1(\tau - 2) = -\frac{c}{2a} \log(2\pi) + \frac{c(\tau - 1)}{2a} \log \frac{2c}{a} + \frac{c}{a} \log \left[ \Gamma \left( \frac{\tau}{2} \right) \right]. \quad (4.26)$$

With  $f_1$  and  $g_1$  known, (4.15) and (4.16) lead to

$$\tilde{P} = -\frac{c}{a} \log 2\pi - \frac{c\tau}{a} \log \frac{2c}{a} + \frac{c}{a} \left[ \log \left\{ \Gamma \left( 1 + \frac{\tau - x}{2} \right) \right\} + \log \left\{ \Gamma \left( \frac{\tau + x}{2} \right) \right\} \right], \quad (4.27)$$

$$\tilde{U} = \frac{c}{a} \log x - \frac{c}{a}(1-x) \log \frac{2c}{a} + \frac{c}{a} \left[ -\log \left\{ \Gamma \left( 1 + \frac{\tau - x}{2} \right) \right\} + \log \left\{ \Gamma \left( \frac{\tau + x}{2} \right) \right\} \right], \quad (4.28)$$

and with  $\tilde{\psi}$  given by (4.10), the solution in the layer is now complete.

We note that  $g_1(\tau)$  has a logarithmic singularity at  $\tau = 0$  while  $f_1$  remains regular there; see equations (A17) and (A19) in Appendix A2. Therefore, (4.27) shows that as  $\tau$  decreases from  $\infty$ ,  $\tilde{P}$  remains bounded until  $\tau = 0$ , when it becomes singular at  $x = 0$ . Likewise, (4.28) shows that  $\tilde{U}$  is singular only at  $x = 0$ . The implication is that for  $0 < x < 1$  the solution remains bounded at  $\tau = 0$ . Thus the layer has resolved the singular behavior (in  $U$  across the slot) it inherited from the induction solution, and only the singularity at the wall remains.

## 5. Corner

In the corner region,  $x = \alpha X$ ,  $t_c - t = \alpha\tau$  and  $\psi$  vanishes at leading order. We set  $\psi = \alpha\hat{\psi}$ , and with  $P = \hat{P}$  and  $U = \hat{U}$ , the induction equations (3.6), (3.13) and (3.14) read

$$\hat{P}_X - \alpha^2 \hat{U}_\tau = 0, \quad (5.1)$$

$$\hat{U}_X - \hat{P}_\tau = \frac{1}{\psi}, \tag{5.2}$$

$$\hat{\psi}_\tau + (\gamma - 1)\hat{\psi}\hat{P}_\tau = 1. \tag{5.3}$$

This equation set is precisely the same as the induction-equation set from which it has just been derived, except that the coordinates  $X$  and  $\tau$  are stretched versions of  $x$  and  $t$ , the rigid-wall boundary condition at  $x = 1$  is now replaced by matching (as  $X \rightarrow \infty$ ) with solution in the interior layer, and initial conditions as  $\tau \rightarrow \infty$  are provided by the near-wall blowup behavior developed in (3.33), (3.35 b) and (3.40). These are

$$\psi \sim \alpha \left( \tau + \frac{aX}{c} \right) - \alpha^2 \log \alpha (\gamma - 1)\tau \left( \frac{c\tau}{2a} + X \right) + \alpha^2 (\gamma - 1)\tau \left( \frac{c\tau}{4a} - \frac{c\tau}{2a} \log \frac{c\tau}{a} - X \log \frac{c\tau}{a} + X \right), \tag{5.4}$$

$$P \sim P(t_c) + \alpha \left( \frac{c\tau}{a} \log \alpha + \frac{c\tau}{a} \log \frac{c\tau}{a} - \frac{c\tau}{a} \right), \tag{5.5}$$

$$U \sim \frac{c}{a} \log \left( 1 + \frac{aX}{c\tau} \right) + \frac{c}{a} \alpha \log \alpha \left\{ X - \frac{\gamma - 1}{2} \frac{X}{1 + aX/c\tau} + (\gamma - 1) \frac{c\tau}{a} \log \left( 1 + \frac{aX}{c\tau} \right) \right\} + \frac{c}{a} \alpha \left\{ X \log \frac{c\tau}{a} - \frac{\gamma - 1}{2} \frac{X}{1 + aX/c\tau} \left( \log \frac{c\tau}{a} - \frac{3}{2} \right) + (\gamma - 1) \frac{c\tau}{a} \left( \log \frac{c\tau}{a} - 1 \right) \log \left( 1 + \frac{aX}{c\tau} \right) \right\}. \tag{5.6}$$

Guided by the above conditions we seek the solution

$$\hat{\psi} \sim \tau + \frac{aX}{c} + \alpha \log \alpha \hat{\psi}_{10} + \alpha \hat{\psi}_{11}, \tag{5.7}$$

$$\hat{P} \sim P(t_c) + \frac{c\tau}{a} \alpha \log \alpha + \alpha \hat{P}_1, \tag{5.8}$$

$$\hat{U} \sim \frac{c}{a} \log \left( 1 + \frac{aX}{c\tau} \right) + \alpha \log \alpha \hat{U}_{10} + \alpha \hat{U}_{11}. \tag{5.9}$$

From (5.1) we obtain  $\hat{P}_{1x} = 0$  so that  $\hat{P}_1 = \hat{P}_1(\tau)$ . We are now ready to match with the interior layer. The above expression for  $\hat{U}$ , upon truncation at order unity followed by expansion to order unity in the layer variables  $(x, \tau)$ , yields

$$U \sim \frac{c}{a} \log \left( 1 + \frac{aX}{c\tau} \right) \sim -\frac{c}{a} \log \alpha - \frac{c}{a} \log \frac{c\tau}{a} + \frac{c}{a} \log x.$$

The corresponding layer solution (4.16), when expanded to order unity as  $x \rightarrow 0$ , becomes

$$U \sim -\frac{c}{a}(1 - x) \log \alpha + \tilde{U} \sim -\frac{c}{a}(1 - x) \log \alpha + \frac{c}{a} \log x + f_1(\tau - x) + g_1(\tau + x) \sim -\frac{c}{a} \log \alpha + \frac{c}{a} \log x + f_1(\tau) + g_1(\tau).$$

Then matching leads to the condition

$$f_1(\tau) + g_1(\tau) = -\frac{c}{a} \log \frac{c\tau}{a},$$

which was anticipated in (4.19). Likewise, matching of the corner pressure  $\hat{P}$  from (5.8) with the interior-layer pressure  $\tilde{P}$  from (4.15) shows that

$$\hat{P}_1(\tau) = \tilde{P}(0, \tau) = -f_1(\tau) + g_1(\tau). \tag{5.10}$$

Thus  $\hat{P}$  is determined to order  $\alpha$  while  $\hat{\psi}$  and  $\hat{U}$  are each known only to order unity. In order to determine  $\hat{\psi}$  to order  $\alpha$  we integrate (5.3) to get

$$\hat{\psi} = e^{-(\gamma-1)\hat{P}(\tau)} \left( aX + \int_0^\tau e^{(\gamma-1)\hat{P}(\lambda)} d\lambda \right), \tag{5.11}$$

where  $\hat{P}$  now stands for its own known expansion to order  $\alpha$  and the function of integration  $aX$  has been determined by matching with (5.4) or, perhaps more simply, by comparison with the induction solution (3.19). Equation (5.2) can then be integrated subject to the rigid-wall boundary condition  $\hat{U}(0, \tau) = 0$  to obtain

$$\hat{U} = X \hat{P}_\tau + \frac{1}{a} e^{(\gamma-1)\hat{P}(\tau)} \log \frac{aX + \int_0^\tau e^{(\gamma-1)\hat{P}(\lambda)} d\lambda}{\int_0^\tau e^{(\gamma-1)\hat{P}(\lambda)} d\lambda}. \tag{5.12}$$

Matching with (5.6) is automatic and similarity to the corresponding solution (3.22) in the induction region is worth noting. That the last two expressions represent the corresponding solutions to  $O(\alpha)$  can be seen explicitly by replacing  $\hat{P}$  by (5.8), its expansion to order  $\alpha$ .

In view of the remarks made at the end of the preceding section about the behavior of  $f_1(\tau)$  and  $g_1(\tau)$  as  $\tau \rightarrow 0$ , we observe from (5.10) that  $\hat{P}_1$  becomes logarithmically singular at  $\tau = 0 +$ . Upon making use of the asymptotic expression (A20) from Appendix A2, the behavior of the corner pressure  $P = \hat{P}$  is found to be

$$P = \hat{P} \sim P(t_c) + \alpha \frac{c}{a} \{ -\log(\alpha\tau) + (1 + \tau) \log \alpha - \log \pi \}. \tag{5.13}$$

Upon substituting this expression in (5.11) and (5.12) we are led to the corresponding asymptotic forms of  $\mathcal{T}$  and  $U$ ,

$$\begin{aligned} \mathcal{T} &= -\log \psi = -\log(\alpha \hat{\psi}) \\ &\sim -\log(\alpha\tau) - \log \left( 1 + \frac{aX}{c\tau} \right) - \alpha(\gamma - 1) \frac{\frac{c}{a}}{1 + \frac{aX}{c\tau}} \\ &\quad \left\{ -\tau \ln \alpha \left( \frac{1}{2} + \frac{aX}{c\tau} \right) + 1 + \frac{aX}{c\tau} \ln(\pi\tau) \right\}; \text{ as } \tau \rightarrow 0, \end{aligned} \tag{5.14}$$

and

$$\begin{aligned} U &\sim \frac{c}{a} \log \left( 1 + \frac{aX}{c\tau} \right) + \alpha \log \alpha \frac{c}{a} \tau \left\{ \frac{X}{\tau} - (\gamma - 1) \frac{\frac{X}{2\tau}}{1 + \frac{aX}{c\tau}} + (\gamma - 1) \frac{c}{a} \log \left( 1 + \frac{aX}{c\tau} \right) \right\} \\ &\quad + \alpha \frac{c}{a} \left\{ -\frac{X}{\tau} + (\gamma - 1) \frac{X}{\tau} \frac{\log(\pi\tau) - 1}{1 + \frac{aX}{c\tau}} - (\gamma - 1) \frac{c}{a} \log(\pi\tau) \log \left( 1 + \frac{aX}{c\tau} \right) \right\} \\ &\quad \text{as } \tau \rightarrow 0. \end{aligned} \tag{5.15}$$

The asymptotic form of the solution has a self-similar structure, with  $X/\tau$  the similarity variable. We observe that the expansion (5.13) for  $P$  is disordered when  $\tau$  is exponentially small such that  $\alpha \log(\alpha\tau)$  is of order unity. The solution in the slotwide internal layer treated in Section 4, being bounded as  $\tau \rightarrow 0$ , will remain frozen at this ultrashort time scale, so that we only need focus attention at the now shrinking hotspot developing in the corner region.

### 6. Hot Spot

We shall find that the hot spot has a two-layer structure, consisting of an internal core where  $X = O(\tau)$ , and an outer shell in which  $X = O(\tau/\alpha)$ .

#### 6.1. CORE

We use  $\zeta = X/\tau$  as the spatial coordinate in the core, and define the exponentially short time coordinate  $\sigma > 0$  by means of the transformation

$$\sigma = -\alpha \log(\alpha\tau), \quad \text{or} \quad \tau = \frac{1}{\alpha} e^{-\sigma/\alpha}. \tag{6.1}$$

The induction equations, (3.6)–(3.8), when transformed into the coordinates  $(\zeta, \sigma)$ , become

$$\alpha^2(\alpha U_\sigma + \zeta U_\zeta) + P_\zeta = 0, \tag{6.2}$$

$$U_\zeta + (\alpha P_\sigma + \zeta P_\zeta) = \exp\left(\mathcal{T} - \frac{\sigma}{\alpha}\right), \tag{6.3}$$

$$\alpha \mathcal{T}_\sigma + \zeta \mathcal{T}_\zeta - (\gamma - 1)(\alpha P_\sigma + \zeta P_\zeta) = \exp\left(\mathcal{T} - \frac{\sigma}{\alpha}\right). \tag{6.4}$$

The matching conditions for  $\sigma \rightarrow 0$  come from (5.13)–(5.15):

$$P \sim P(t_c) + \frac{c\sigma}{a} + \frac{c}{a}\alpha \log \alpha - \frac{\alpha c}{a} \log \pi, \tag{6.5}$$

$$\mathcal{T} \sim \frac{\sigma}{\alpha} - \log\left(1 + \frac{a\zeta}{c}\right) + (\gamma - 1)\frac{\sigma\zeta}{1 + \frac{a\zeta}{c}} + \alpha \log \alpha (\gamma - 1)\frac{\zeta}{1 + \frac{a\zeta}{c}} - \alpha (\gamma - 1)\frac{\zeta \log \pi + c/a}{1 + \frac{a\zeta}{c}}, \tag{6.6}$$

$$\begin{aligned} U \sim & \frac{c}{a} \log\left(1 + \frac{a\zeta}{c}\right) - (\gamma - 1)\frac{c}{a}\frac{\sigma\zeta}{1 + \frac{a\zeta}{c}} + (\gamma - 1)\frac{c^2}{a^2}\sigma \log\left(1 + \frac{a\zeta}{c}\right) \\ & + \alpha \log \alpha (\gamma - 1)\left\{\frac{c^2}{a^2} \log\left(1 + \frac{a\zeta}{c}\right) - \frac{c}{a}\frac{\zeta}{1 + \frac{a\zeta}{c}}\right\} \\ & \alpha \left\{-\frac{c}{a}\zeta + (\gamma - 1)\frac{c}{a}\frac{\zeta(\log \pi - 1)}{1 + \frac{a\zeta}{c}} - (\gamma - 1)\frac{c^2}{a^2} \log \pi \log\left(1 + \frac{a\zeta}{c}\right)\right\}. \end{aligned} \tag{6.7}$$

Guided by these conditions we can expand the solution as

$$\mathcal{T} \sim \frac{\sigma}{\alpha} + \bar{\mathcal{T}}_0 + \alpha(\log \alpha \bar{\mathcal{T}}_{10} + \bar{\mathcal{T}}_{11}) + \alpha^2(\log^2 \alpha \bar{\mathcal{T}}_{20} + \log \alpha \bar{\mathcal{T}}_{21} + \bar{\mathcal{T}}_{22}), \tag{6.8}$$

$$P \sim \bar{P}_0 + \alpha(\log \alpha \bar{P}_{10} + \bar{P}_{11}) + \alpha^2(\log^2 \alpha \bar{P}_{20} + \log \alpha \bar{P}_{21} + \bar{P}_{22}), \tag{6.9}$$



$$U \sim \bar{U}_0 + \alpha(\log \alpha \bar{U}_{10} + \bar{U}_{11}) + \alpha^2(\log^2 \alpha \bar{U}_{20} + \log \alpha \bar{U}_{21} + \bar{U}_{22}). \quad (6.10)$$

We are interested in  $\mathcal{T}$  and  $U$  only to order unity, and in  $P$  to order  $\alpha$ . However, as we shall see, a complete specification of the solution even to this low order will require the determination of four primary and two secondary functions of integration, thereby necessitating the rather lengthy higher-order treatment given below.

6.1.1. *The case  $O(1)$*

At  $O(1)$  the momentum equation (6.2) yields  $\bar{P}_{0\zeta} = 0$ , whence  $\bar{P}_0 = \bar{P}_0(\sigma)$ . This is the first function of integration. Matching with (6.5) provides the initial condition

$$\bar{P}_0(0) = P(t_c), \quad (6.11)$$

where the constant  $P(t_c)$  was defined in (3.27). The energy equation (6.4) reduces to

$$1 + \zeta \bar{\mathcal{T}}_{0\zeta} = e^{\bar{\mathcal{T}}_0}$$

and has the integral

$$\bar{\mathcal{T}}_0 = -\log(1 + K_0\zeta), \quad (6.12)$$

where  $K_0(\sigma)$  is the second function of integration. Matching with (6.6) as  $\sigma \rightarrow 0$  determines the initial value

$$K_0(0) = a/c. \quad (6.13)$$

The mass equation (6.3) then reduces to

$$\bar{U}_{0\zeta} = e^{\bar{\mathcal{T}}_0},$$

which, subject to the zero-velocity wall condition at  $\zeta = 0$ , integrates to

$$\bar{U}_0 = \frac{1}{K_0} \log(1 + K_0\zeta). \quad (6.14)$$

At this stage the order-unity solution is at hand, except for the unknown functions  $\bar{P}_0(\sigma)$  and  $K_0(\sigma)$ .

6.1.2. *The case  $O(\alpha \log \alpha)$*

In a completely analogous way the solution at  $O(\alpha \log \alpha)$  is found to be

$$\bar{P}_{10} = \bar{P}_{10}(\sigma), \quad \bar{\mathcal{T}}_{10} = \frac{K_{10}\zeta}{1 + K_0\zeta}, \quad \bar{U}_{10} = \frac{K_{10}}{K_0^2} \left( \log(1 + K_0\zeta) - \frac{K_0\zeta}{1 + K_0\zeta} \right), \quad (6.15)$$

where  $\bar{P}_{10}(\sigma)$  and  $K_{10}(\sigma)$  are the third and fourth functions of integration. The initial conditions

$$\bar{P}_{10}(0) = c/a, \quad (6.16)$$

$$K_{10}(0) = \gamma - 1, \quad (6.17)$$

come from matching with (6.5) and (6.6), respectively.

6.1.3. *The case  $O(\alpha)$*

The momentum equation (6.2) again leads to  $\bar{P}_{11} = \bar{P}_{11}(\sigma)$ , the fifth function of integration, with (6.5) providing the initial condition

$$\bar{P}_{11}(0) = -(c/a) \log \pi. \quad (6.18)$$

The energy equation (6.4) reduces to

$$\bar{\mathcal{T}}_{0\sigma} + \zeta \bar{\mathcal{T}}_{11\zeta} - (\gamma - 1) \bar{P}_{0\sigma} = \bar{\mathcal{T}}_{11} e^{\bar{\mathcal{J}}_0},$$

or, upon substitution of the known quantities computed above, to

$$\frac{\partial}{\partial \zeta} \left( \frac{1 + K_0 \zeta}{\zeta} \bar{\mathcal{T}}_{11} \right) = (\gamma - 1) \frac{1 + K_0 \zeta}{\zeta^2} \bar{P}_{0\sigma} + \frac{K_{0\sigma}}{\zeta}.$$

The solution for  $\bar{\mathcal{T}}_{11}$  will, in general, be singular like  $\zeta \log \zeta$  at  $\zeta = 0$  unless the right-hand side carries no terms of order  $1/\zeta$  in its small- $\zeta$  expansion. Enforcing this condition leads to the relation

$$K_{0\sigma} + (\gamma - 1) K_0 \bar{P}_{0\sigma} = 0 \quad (6.19)$$

between two of the unknown functions,  $K_0(\sigma)$  and  $\bar{P}_0(\sigma)$ . Then the above equation for  $\bar{\mathcal{T}}_{11}$  integrates to yield

$$\bar{\mathcal{T}}_{11} = -\frac{\gamma - 1}{1 + K_0 \zeta} \bar{P}_{0\sigma} + \frac{K_{11} \zeta}{1 + K_0 \zeta}, \quad (6.20)$$

where  $K_{11}(\sigma)$  is the sixth (and last) in the list of unknown functions of  $\sigma$ . The initial condition

$$K_{11}(0) = -(\gamma - 1) \log \pi \quad (6.21)$$

comes from matching with (6.6). At this order the mass equation (6.3) has the reduced form

$$\bar{U}_{11\zeta} = -\bar{P}_{0\sigma} + \frac{1}{(1 + K_0 \zeta)^2} (-(\gamma - 1) \bar{P}_{0\sigma} + K_{11} \zeta),$$

which, subject to the zero-velocity condition at the wall, integrates to yield

$$\bar{U}_{11} = -\bar{P}_{0\sigma} \zeta - (\gamma - 1) \frac{\bar{P}_{0\sigma} \zeta}{(1 + K_0 \zeta)} + \frac{K_{11}}{K_0^2} \left( \log(1 + K_0 \zeta) - \frac{K_0 \zeta}{1 + K_0 \zeta} \right). \quad (6.22)$$

At this stage only one constraint, (6.19), among the six unknowns  $K_0$ ,  $K_{10}$ ,  $K_{11}$ ,  $\bar{P}_0$ ,  $\bar{P}_{10}$  and  $\bar{P}_{11}$ , all functions of  $\sigma$ , has been obtained. Additional constraints, as we show below, emerge upon carrying the solution to higher orders and requiring that these higher-order terms satisfy appropriate regularity conditions.

#### 6.1.4. *The case $O(\alpha^2 \log^2 \alpha)$*

From the momentum equation (6.2),  $\bar{P}_{20} = \bar{P}_{20}(\sigma)$ . Then the energy equation (6.4) yields

$$\zeta \bar{\mathcal{T}}_{20\zeta} - e^{\bar{\mathcal{J}}_0} \bar{\mathcal{T}}_{20} = \frac{1}{2} e^{\bar{\mathcal{J}}_0} \bar{\mathcal{T}}_{10}^2.$$

Upon substituting for  $\bar{\mathcal{T}}_0$  and  $\bar{\mathcal{T}}_{10}$  followed by a rearrangement, the above equation reads

$$\left( \frac{1 + K_0 \zeta}{\zeta} \bar{\mathcal{T}}_{20} \right)_\zeta = \frac{K_{10}^2}{2(1 + K_0 \zeta)^2},$$

and integrates to yield

$$\bar{\mathcal{J}}_{20} = -\frac{K_{10}^2}{2K_0} \frac{\zeta}{(1 + K_0\zeta)^2} + K_{20} \frac{\zeta}{1 + K_0\zeta}, \tag{6.23}$$

where  $K_{20}(\sigma)$  is a function of integration. The mass equation (6.3) reduces at this order to

$$\bar{U}_{20\zeta} = e^{\bar{\mathcal{J}}_0} \left( \bar{\mathcal{J}}_{20} + \frac{1}{2} e^{\bar{\mathcal{J}}_0} \bar{\mathcal{J}}_{10}^2 \right) = \zeta \bar{\mathcal{J}}_{20\zeta}.$$

Upon integration subject to  $\bar{U}_{20}(0, \sigma) = 0$  we get

$$\begin{aligned} \bar{U}_{20} = & -\frac{K_{10}^2}{2K_0} \frac{\zeta^2}{(1 + K_0\zeta)^2} + K_{20} \frac{\zeta^2}{1 + K_0\zeta} + \frac{K_{10}^2}{2K_0^3} \left( \log(1 + K_0\zeta) - \frac{K_0\zeta}{1 + K_0\zeta} \right) \\ & + \frac{K_{20}}{K_0^2} \{K_0\zeta - \log(1 + K_0\zeta)\}. \end{aligned} \tag{6.24}$$

No new constraints emerge at this stage.

6.1.5. *The case  $O(\alpha^2 \log \alpha)$*

The momentum equation (6.2) continues to imply the spatial independence of pressure, *i.e.*,  $\bar{P}_{21} = \bar{P}_{21}(\sigma)$ . The energy equation (6.4) then reduces to

$$\zeta \bar{\mathcal{J}}_{21\zeta} - e^{\bar{\mathcal{J}}_0} \bar{\mathcal{J}}_{21} = -\bar{\mathcal{J}}_{10\sigma} + (\gamma - 1) \bar{P}_{10\sigma} + e^{\bar{\mathcal{J}}_0} \bar{\mathcal{J}}_{11} \bar{\mathcal{J}}_{10}.$$

Upon substitution of known expressions for  $\bar{\mathcal{J}}_0$ ,  $\bar{\mathcal{J}}_{10}$  and  $\bar{\mathcal{J}}_{11}$ , the above equation can be rewritten as

$$\begin{aligned} \frac{\partial}{\partial \zeta} \left( \frac{1 + K_0\zeta}{\zeta} \bar{\mathcal{J}}_{21} \right) &= \frac{1 + K_0\zeta}{\zeta^2} \{-\bar{\mathcal{J}}_{10\sigma} + (\gamma - 1) \bar{P}_{10\sigma}\} + \frac{1}{\zeta^2} \bar{\mathcal{J}}_{10} \bar{\mathcal{J}}_{11} \\ &= \frac{1 + K_0\zeta}{\zeta^2} \left\{ -\frac{K_{10\sigma} \zeta}{1 + K_0\zeta} + \frac{K_{10} K_{0\sigma} \zeta^2}{(1 + K_0\zeta)^2} + (\gamma - 1) \bar{P}_{10\sigma} \right\} + \\ &\quad \frac{K_{10}}{\zeta(1 + K_0\zeta)^2} \{-(\gamma - 1) \bar{P}_{0\sigma} + K_{11}\zeta\}. \end{aligned}$$

Regularity of  $\bar{\mathcal{J}}_{21}$  at  $\zeta = 0$  requires elimination of  $O(1/\zeta)$  terms in the expansion of the right-hand side as  $\zeta \rightarrow 0$ . This leads to the second constraint

$$-K_{10\sigma} + (\gamma - 1) \bar{P}_{10\sigma} K_0 - (\gamma - 1) K_{10} \bar{P}_{0\sigma} = 0. \tag{6.25}$$

6.1.6. *The case  $O(\alpha^2)$*

From the momentum equation (6.2) we see that pressure gradients now enter the picture, *i.e.*,

$$\begin{aligned} \bar{P}_{22\zeta} &= -\zeta \bar{U}_{0\zeta} \\ &= -\frac{\zeta}{1 + K_0\zeta}, \end{aligned}$$

where we have used (6.14). An integration leads to

$$\bar{P}_{22} = -\frac{\zeta}{K_0} + \frac{1}{K_0^2} \log(1 + K_0\zeta) + \bar{\mathcal{P}}_{22}(\sigma), \tag{6.26}$$

where  $\bar{\mathcal{P}}_{22}(\sigma)$  is the function of integration. The energy equation (6.4) reduces to

$$\begin{aligned}\zeta \bar{\mathcal{T}}_{22\zeta} - e^{\bar{\mathcal{T}}_0} \bar{\mathcal{T}}_{22} &= -\bar{\mathcal{T}}_{11\sigma} + (\gamma - 1)\{\bar{P}_{11\sigma} + \zeta \bar{P}_{22\zeta}\} + \frac{1}{2}e^{\bar{\mathcal{T}}_0} \bar{\mathcal{T}}_{11}^2 \\ &= -\bar{\mathcal{T}}_{11\sigma} + (\gamma - 1)\{\bar{P}_{11\sigma} - \zeta^2 \bar{U}_{0\zeta}\} + \frac{1}{2}e^{\bar{\mathcal{T}}_0} \bar{\mathcal{T}}_{11}^2.\end{aligned}$$

Upon substitution of known expressions for  $\bar{\mathcal{T}}_0$ ,  $\bar{\mathcal{T}}_{11}$  and  $\bar{U}_0$ , the above equation can be rearranged into

$$\begin{aligned}\frac{\partial}{\partial \zeta} \left( \frac{1 + K_0 \zeta}{\zeta} \bar{\mathcal{T}}_{22} \right) &= \frac{1}{\zeta^2} \left\{ (\gamma - 1) \bar{P}_{0\sigma\sigma} - (\gamma - 1) \bar{P}_{0\zeta} K_{0\zeta} \frac{\zeta}{1 + K_0 \zeta} - K_{11\sigma} \zeta + K_{11} K_{0\sigma} \frac{\zeta^2}{1 + K_0 \zeta} \right\} \\ &\quad + \frac{1}{2\zeta^2 (1 + K_0 \zeta)^2} \{ (\gamma - 1)^2 \bar{P}_{0\sigma}^2 + K_{11}^2 \zeta^2 - 2(\gamma - 1) \bar{P}_{0\sigma} K_{11} \zeta \} \\ &\quad + (\gamma - 1) \bar{P}_{11\sigma} \frac{1 + K_0 \zeta}{\zeta^2} - (\gamma - 1).\end{aligned}$$

As above, regularity at  $\zeta = 0$  requires that the right-hand side be devoid of any  $O(1/\zeta)$  terms as  $\zeta \rightarrow 0$ , thus providing the third condition

$$-K_{11\sigma} + (\gamma - 1) \bar{P}_{11\sigma} K_0 - (\gamma - 1) \bar{P}_{0\sigma} K_{11} - (\gamma - 1) \bar{P}_{0\sigma} K_{0\sigma} - (\gamma - 1)^2 \bar{P}_{0\sigma}^2 K_0 = 0. \quad (6.27)$$

In Equations (6.19), (6.25) and (6.27) we now have three constraints for the six unknowns identified earlier, derived by enforcing regularity at the hot wall. To derive the remaining three constraints we turn to the shell region in which  $\zeta = O(1/\alpha)$ . We shall find that the additional constraints come from enforcement of regularity along a characteristic ray coming into the hot spot. The need for examining the shell is also suggested by the algebraic growth in  $\bar{U}_{11}$ , Equation (6.22), which causes the expansion (6.10) for  $U$  to become disordered.

## 6.2. SHELL

In the shell we continue to employ the time coordinate  $\sigma$  but introduce  $\eta = \alpha \zeta$  as the new spatial coordinate. Then equations (6.2)–(6.4) assume the form

$$\alpha U_\sigma + \eta U_\eta + \frac{1}{\alpha} P_\eta = 0, \quad (6.28)$$

$$U_\eta + P_\sigma + \frac{1}{\alpha} \eta P_\eta = \frac{1}{\alpha} \exp\left(\mathcal{T} - \frac{\sigma}{\alpha}\right), \quad (6.29)$$

$$\alpha \mathcal{T}_\sigma + \eta T_\eta - (\gamma - 1)(\alpha P_\sigma + \eta P_\eta) = \exp\left(\mathcal{T} - \frac{\sigma}{\alpha}\right). \quad (6.30)$$

Elimination of  $P_\eta$  from (6.28) and (6.29) yields the following, more convenient, alternative to the mass equation (6.29):

$$(\eta^2 - 1)U_\eta = P_\sigma - \alpha \eta U_\sigma - \frac{1}{\alpha} \exp\left(\mathcal{T} - \frac{\sigma}{\alpha}\right). \quad (6.31)$$

To obtain the necessary matching conditions as  $\eta \rightarrow 0$ , we turn to the the core solution (6.8)–(6.10) and consider each variable in turn. From (6.8) we take  $\mathcal{T}$  to order  $\alpha$ , and expand it to order  $\alpha$  in the ‘shell’ limit  $\alpha \rightarrow 0$  with  $\eta$  fixed, to get

$$\mathcal{T} \sim \frac{\sigma}{\alpha} + \log \alpha - \log(K_0 \eta) + \alpha \log \alpha \frac{K_{10}}{K_0} + \alpha \frac{1}{K_0} \left( K_{11} - \frac{1}{\eta} \right). \quad (6.32)$$

From (6.9) we take  $P$  to order  $\alpha^2$  and expand it to order  $\alpha^2$  in the shell limit. The result is

$$P \sim \bar{P}_0(\sigma) + \alpha \log \alpha \bar{P}_{10}(\sigma) + \alpha \left( \bar{P}_{11}(\sigma) - \frac{\eta}{K_0} \right) + \alpha^2 \log^2 \alpha \bar{P}_{20}(\sigma) + \alpha^2 \log \alpha \left( \bar{P}_{21}(\sigma) - \frac{1}{K_0^2} \right) + \alpha^2 \left( \bar{P}_{22}(\sigma) + \frac{1}{K_0^2} \log(K_0 \eta) \right). \quad (6.33)$$

Finally, from (6.10) we take  $U$  to order  $\alpha$ , and expand it to order  $\alpha^2$  in the shell limit to obtain

$$U \sim -\frac{1}{K_0} \log \alpha + \frac{1}{K_0} \{ \log(K_0 \eta) - K_0 \bar{P}_{0\sigma} \eta \} - \alpha \log^2 \alpha \frac{K_{10}}{K_0} + \alpha \log \alpha \frac{1}{K_0^2} \{ K_{10} \log(K_0 \eta) - K_{10} - K_{11} \} + \alpha \frac{1}{K_0^2} \left( \frac{1}{\eta} - (\gamma - 1) K_0 \bar{P}_{0\sigma} + K_{11} \{ \log(K_0 \eta) - 1 \} \right). \quad (6.34)$$

Guided by these conditions the shell solution is expanded as

$$\mathcal{T} \sim \frac{\sigma}{\alpha} + \log \alpha + T_0^* + \alpha \log \alpha \mathcal{T}_{10}^* + \alpha \mathcal{T}_{11}^*, \quad (6.35)$$

$$P \sim \bar{P}_0(\sigma) + \alpha \log \alpha \bar{P}_{10}(\sigma) + \alpha P_{11}^* + \alpha^2 \log^2 \alpha P_{20}^* + \alpha^2 \log \alpha P_{21}^* + \alpha^2 P_{22}^*, \quad (6.36)$$

$$U \sim -\frac{1}{K_0} \log \alpha + U_0^* + \alpha \log^2 \alpha U_{10}^* + \alpha \log \alpha U_{11}^* + \alpha U_{12}^*. \quad (6.37)$$

As in the core, our interest in the shell also extends only to order unity in  $\mathcal{T}$  and  $U$  and to order  $\alpha$  in  $P$ .

### 6.2.1. The case $O(1)$

Substitution in (6.28), (6.30) and (6.31) yields the following reduced equations at order unity:

$$\eta U_{0\eta}^* + P_{11\eta}^* = 0, \quad (6.38)$$

$$1 + \eta \mathcal{T}_{0\eta}^* = 0. \quad (6.39)$$

$$(\eta^2 - 1) U_{0\eta}^* = \bar{P}_{0\sigma} - e^{\mathcal{T}_0^*}. \quad (6.40)$$

Equation (6.39), upon integration and matching with (6.32), yields

$$\mathcal{T}_0^* = -\log(K_0 \eta). \quad (6.41)$$

Substitution of the above expression for  $\mathcal{T}_0^*$  in (6.40) leads to

$$(\eta^2 - 1) U_{0\eta}^* = \bar{P}_{0\sigma} - \frac{1}{K_0 \eta}. \quad (6.42)$$

Regularity on the (incoming characteristic) line  $\eta = 1$  imposes the condition

$$K_0 \bar{P}_{0\sigma} = 1. \quad (6.43)$$

This is the fourth in the list of the six regularity constraints that we seek. Equations (6.19) and (6.43) serve to determine two of the six unknown functions,  $\bar{P}_0(\sigma)$  and  $K_0(\sigma)$ . These two equations simplify to

$$K_{0\sigma} = -(\gamma - 1), \quad \bar{P}_{0\sigma} = \frac{1}{K_0}.$$

Integration, subject to the initial conditions in (6.11) and (6.13), yields

$$K_0 = \frac{a}{c} - (\gamma - 1)\sigma \equiv (\gamma - 1)(\sigma_0 - \sigma), \tag{6.44}$$

$$\bar{P}_0 = P(t_c) - \frac{1}{\gamma - 1} \log(1 - \sigma/\sigma_0), \tag{6.45}$$

where

$$\sigma_0 \equiv \frac{a}{(\gamma - 1)c}. \tag{6.46}$$

We can now complete the solution. In view of (6.43), Equation (6.42) reduces to

$$(\eta^2 - 1)U_{0\eta}^* = \frac{1}{K_0} - \frac{1}{K_0\eta},$$

and integrates to

$$U_0^* = \frac{1}{K_0} \{ \log(K_0\eta) - \log(1 + \eta) \}, \tag{6.47}$$

where matching with (6.34) has been applied. Then, integration of (6.38) followed by matching with (6.33) yields

$$P_{11}^* = \bar{P}_{11}(\sigma) - \frac{1}{K_0} \log(1 + \eta). \tag{6.48}$$

### 6.2.2. *The case $O(\alpha \log^2 \alpha)$*

At this order (6.30) is satisfied identically while (6.31) and (6.28) reduce, respectively, to

$$(\eta^2 - 1)U_{10\eta}^* = 0, \quad P_{20\eta}^* + \eta U_{10\eta}^* = 0.$$

Upon integration and matching with (6.34) and (6.32) we obtain

$$U_{10}^* = -\frac{K_{10}(\sigma)}{K_0^2(\sigma)}, \tag{6.49}$$

$$P_{20}^* = \bar{P}_{20}(\sigma). \tag{6.50}$$

No new constraints emerge.

### 6.2.3. *The case $O(\alpha \log \alpha)$*

At  $O(\alpha \log \alpha)$  the reduced versions of (6.28), (6.30), and (6.31) are

$$P_{21\eta}^* + \eta U_{11\eta}^* + \frac{K_{0\sigma}}{K_0^2} = 0, \tag{6.51}$$

$$\eta T_{10\eta}^* = 0, \quad (6.52)$$

$$(\eta^2 - 1)U_{11\eta}^* = \bar{P}_{10\sigma} - \frac{K_{0\sigma}}{K_0^2}\eta - e^{\mathcal{J}_0^*} \mathcal{J}_{10}^*. \quad (6.53)$$

Upon integration and matching with (6.32), (6.52) yields

$$\mathcal{J}_{10}^* = \frac{K_{10}(\sigma)}{K_0(\sigma)}. \quad (6.54)$$

Then (6.53) can be written as

$$(\eta^2 - 1)U_{11\eta}^* = \bar{P}_{10\sigma} - \frac{K_{0\sigma}}{K_0^2}\eta - \frac{K_{10}}{K_0^2\eta}. \quad (6.55)$$

Imposition of regularity at  $\eta = 1$  leads to

$$\bar{P}_{10\sigma} = \frac{K_{0\sigma} + K_{10}}{K_0^2}. \quad (6.56)$$

This is the fifth regularity condition of the set of six, and when solved in conjunction with Equation (6.25) and initial conditions (6.16) and (6.17) yields

$$\bar{P}_{10} = \frac{1 + \log(1 - \sigma/\sigma_0)}{(\gamma - 1)(\sigma_0 - \sigma)}, \quad (6.57)$$

$$K_{10} = (\gamma - 1)\{1 + \log(1 - \sigma/\sigma_0)\}. \quad (6.58)$$

Now (6.55) can be rearranged as

$$U_{11\eta}^* = -\frac{K_{0\sigma} + K_{10}}{K_0^2} \frac{1}{1 + \eta} + \frac{K_{10}}{K_0^2\eta},$$

and integrated to obtain

$$U_{11}^* = -\frac{K_{0\sigma} + K_{10}}{K_0^2} \log(1 + \eta) + \frac{K_{10}}{K_0^2} \log(K_0\eta) - \frac{K_{10} + K_{11}}{K_0^2}, \quad (6.59)$$

where matching with (6.34) has been applied. We can now integrate (6.51) subject to matching with (6.33) and get

$$P_{21}^* = -\frac{K_{0\sigma} + K_{10}}{K_0^2} \log(1 + \eta) - \frac{1}{K_0^2} + \bar{P}_{21}(\sigma), \quad (6.60)$$

thus completing the solution at order  $\alpha \log \alpha$ .

#### 6.2.4. The case $O(\alpha)$

At this order the reduced versions of (6.28), (6.30), and (6.31) are

$$P_{22\eta}^* + \eta U_{12\eta}^* + U_{0\sigma}^* = 0, \quad (6.61)$$

$$\eta T_{11\eta}^* = -\mathcal{J}_{0\sigma}^* + (\gamma - 1)\bar{P}_{0\sigma} + (\gamma - 1)\eta P_{11\eta}^* + e^{\mathcal{J}_0^*}, \quad (6.62)$$

$$(\eta^2 - 1)U_{12\eta}^* = \bar{P}_{11\sigma} - \eta U_{0\sigma}^* - e^{\mathcal{J}_0^*} \mathcal{J}_{11}^*. \quad (6.63)$$

Upon substitution of known expressions for  $\mathcal{T}_0^*$  and  $P_{11}^*$  on the right-hand side, (6.62) transforms into

$$\eta T_{11\eta}^* = \frac{K_{0\sigma}}{K_0} + (\gamma - 1)\bar{P}_{0\sigma} - (\gamma - 1)\frac{\eta}{K_0(1 + \eta)} + \frac{1}{K_0\eta}. \tag{6.64}$$

The first two terms on the right-hand side above cancel in view of the regularity condition (6.19). The remaining equation can be integrated subject to the matching requirement imposed by (6.32), leading to

$$T_{11}^* = -\frac{\gamma - 1}{K_0} \log(1 + \eta) - \frac{1}{K_0\eta} + \frac{K_{11}}{K_0}. \tag{6.65}$$

Then, upon substituting the relevant expressions for the known quantities on the right-hand side, we can rewrite (6.63) as

$$(\eta^2 - 1)U_{12\eta}^* = \frac{K_{0\sigma}}{K_0^2} \{ (1 - \eta) \log(1 + \eta) + \eta \log(K_0\eta) - \eta \} + \bar{P}_{11\sigma} - \frac{1}{K_0^2\eta} \left( K_{11} - \frac{1}{\eta} - (\gamma - 1) \log(1 + \eta) \right). \tag{6.66}$$

Regularity of solution at  $\eta = 1$  forces the requirement

$$\bar{P}_{11\sigma} = \frac{K_{0\sigma}}{K_0^2} (1 - \log K_0) + \frac{1}{K_0^2} \{ K_{11} - 1 - (\gamma - 1) \log 2 \}. \tag{6.67}$$

This is the last regularity condition of the set of six, and when solved in conjunction with condition (6.27) and initial conditions (6.18) and (6.21) yields, after considerable algebra,

$$\bar{P}_{11} = -\frac{1}{2(\gamma - 1)(\sigma_0 - \sigma)} \left[ \log^2(1 - \sigma/\sigma_0) - \frac{2Q}{\gamma - 1} \log(1 - \sigma/\sigma_0) + 2 \log \pi \right], \tag{6.68}$$

$$K_{11} = -\frac{\gamma - 1}{2} \left[ \log^2(1 - \sigma/\sigma_0) - \frac{2Q}{\gamma - 1} \log(1 - \sigma/\sigma_0) + 2 \log \pi \right], \tag{6.69}$$

where

$$Q = 1 + (\gamma - 1)[1 - \log\{(\gamma - 1)\sigma_0/2\}]. \tag{6.70}$$

The solution in both the core and the shell of the hot spot is now complete to the desired order. In particular, the six  $\sigma$ -dependent functions  $K_0$ ,  $K_{10}$ ,  $K_{11}$  and  $\bar{P}_0$ ,  $\bar{P}_{10}$  and  $\bar{P}_{11}$ , have all been identified. Of these,  $K_{10}$  and  $K_{11}$  are secondary, in that they do not appear in the solution to the order sought. However, these were coupled with the four primary functions, and hence the need for obtaining the six constraints. For convenience the four primary functions are collected below.

$$K_0 = \frac{a}{c} - (\gamma - 1)\sigma \equiv (\gamma - 1)(\sigma_0 - \sigma), \tag{6.71}$$

$$\bar{P}_0 = P(t_c) - \frac{1}{\gamma - 1} \log(1 - \sigma/\sigma_0), \tag{6.72}$$

$$\bar{P}_{10} = \frac{1 + \log(1 - \sigma/\sigma_0)}{(\gamma - 1)(\sigma_0 - \sigma)}, \tag{6.73}$$

$$\bar{P}_{11} = -\frac{1}{2(\gamma - 1)(\sigma_0 - \sigma)} \left[ \log^2(1 - \sigma/\sigma_0) - \frac{2Q}{\gamma - 1} \log(1 - \sigma/\sigma_0) + 2 \log \pi \right], \tag{6.74}$$



We observe that  $K_0 \rightarrow 0$  while the other three functions are unbounded as  $\sigma \rightarrow \sigma_0 -$ . Also gathered below are the solutions in the core and shell regions in which these functions appear.

6.2.5. *Core Solution*

$$\begin{aligned} \mathcal{T} &\sim \frac{\sigma}{\alpha} + \bar{\mathcal{T}}_0 \\ &= \frac{\sigma}{\alpha} - \log(1 + K_0\zeta), \end{aligned} \tag{6.75}$$

$$P \sim \bar{P}_0 + \alpha(\log \alpha \bar{P}_{10} + \bar{P}_{11}), \tag{6.76}$$

$$\begin{aligned} U &\sim \bar{U}_0 \\ &= \frac{1}{K_0} \log(1 + K_0\zeta). \end{aligned} \tag{6.77}$$

6.2.6. *Shell Solution*

$$\begin{aligned} \mathcal{T} &\sim \frac{\sigma}{\alpha} + \log \alpha + T_0^* \\ &= \frac{\sigma}{\alpha} + \log \alpha - \log(K_0\eta), \end{aligned} \tag{6.78}$$

$$P \sim \bar{P}_0 + \alpha \log \alpha \bar{P}_{10} + \alpha \left\{ \bar{P}_{11} - \frac{1}{K_0} \log(1 + \eta) \right\}, \tag{6.79}$$

$$\begin{aligned} U &\sim -\frac{1}{K_0} \log \alpha + U_0^* \\ &= -\frac{1}{K_0} \log \alpha + \frac{1}{K_0} [\log(K_0\eta) - \log(1 + \eta)]. \end{aligned} \tag{6.80}$$

It is also useful to write down the composite hot-spot solution.

6.2.7. *Composite Solution*

$$\mathcal{T} \sim \frac{\sigma}{\alpha} - \log \left( 1 + \frac{K_0\eta}{\alpha} \right), \tag{6.81}$$

$$P \sim \bar{P}_0 + \alpha \log \alpha \bar{P}_{10} + \alpha \left\{ \bar{P}_{11} - \frac{1}{K_0} \log(1 + \eta) \right\}, \tag{6.82}$$

$$U \sim \frac{1}{K_0} \left[ \log \left( 1 + \frac{K_0\eta}{\alpha} \right) - \log(1 + \eta) \right]. \tag{6.83}$$

Figure 3 shows a good agreement between the profiles of  $\mathcal{T}$  according to the composite solution obtained above, and the numerical solution, at  $t = 0.81352$ . In drawing the graph of the asymptotic solution we have employed the numerically obtained value of the blowup time,  $t_c = 0.81712$ . Correspondingly,  $\sigma = 1.12536 < \sigma_0 = 1.43587$ , indicating that the transition stage, discussed below, has not yet been reached.

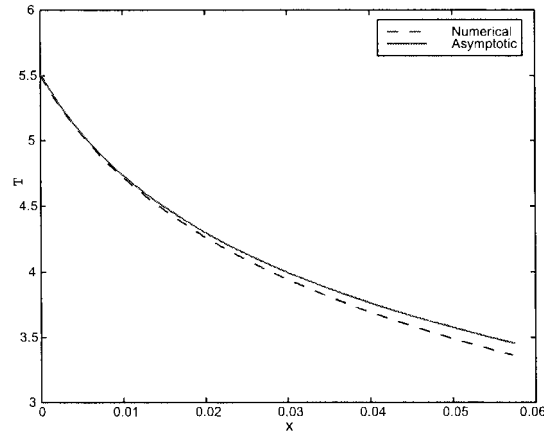


Figure 3. A comparison of the composite hot-spot solution, and the numerical solution, for the profile of  $\mathcal{T}$  at  $t = 0.81352$  for  $\gamma = 1.4$ ,  $a = 1$  and  $\alpha = 0.2$ .

### 7. Transition

In view of the already-noted behavior of the functions appearing in (6.71)–(6.74), the above expansions for the composite solution in the hot spot break down as  $\sigma \rightarrow \sigma_0 -$ . We now show that the next stage of evolution is a transition stage, in which  $\alpha$  completely disappears from the governing equations and the full Clarke equations emerge. For a precise specification of the transition time scale and the relevant matching conditions, consider first the composite  $P$ -expansion (6.82) in the hot spot. Upon substituting from (6.71)–(6.74) the appropriate expressions for the functions of  $\sigma$  appearing in this expansion, we obtain

$$\begin{aligned}
 P \sim & P(t_c) - \frac{1}{\gamma - 1} \log(1 - \sigma/\sigma_0) + \alpha \log \alpha \frac{1 + \log(1 - \sigma/\sigma_0)}{(\gamma - 1)(\sigma_0 - \sigma)} \\
 & - \alpha \frac{1}{2(\gamma - 1)(\sigma_0 - \sigma)} \left[ \log^2(1 - \sigma/\sigma_0) - \frac{2Q}{\gamma - 1} \log(1 - \sigma/\sigma_0) + 2 \log \pi + 2 \log(1 + \eta) \right].
 \end{aligned}
 \tag{7.1}$$

For  $\sigma_0 - \sigma = O(1)$  this expression can be rewritten in the following form:

$$\begin{aligned}
 P \sim & P(t_c) - \frac{1}{\gamma - 1} \log(1 - \sigma/\sigma_0 - \alpha \log^2 \alpha / 2\sigma_0 - \mu \alpha \log \alpha / \sigma_0) \\
 & - \alpha \log^2 \alpha \frac{1}{2(\gamma - 1)(\sigma_0 - \sigma)} - \alpha \log \alpha \frac{\mu}{(\gamma - 1)(\sigma_0 - \sigma)} \\
 & + \alpha \log \alpha \frac{1 + \log(1 - \sigma/\sigma_0 - \alpha \log^2 \alpha / 2\sigma_0 - \mu \alpha \log \alpha / \sigma_0)}{(\gamma - 1)(\sigma_0 - \sigma)} \\
 & - \alpha \frac{1}{2(\gamma - 1)(\sigma_0 - \sigma)} \left[ \log^2(1 - \sigma/\sigma_0 - \alpha \log^2 \alpha / 2\sigma_0 - \mu \alpha \log \alpha / \sigma_0) \right. \\
 & \left. - \frac{2Q}{\gamma - 1} \log(1 - \sigma/\sigma_0 - \alpha \log^2 \alpha / 2\sigma_0 - \mu \alpha \log \alpha / \sigma_0) + 2 \log \pi + 2 \log(1 + \eta) \right].
 \end{aligned}$$

The above expression was obtained by altering, in (7.1), the argument of each logarithm from  $1 - \sigma/\sigma_0$  to  $1 - \sigma/\sigma_0 - \alpha \log^2 \alpha / 2\sigma_0 - \mu \alpha \log \alpha / \sigma_0$ , and by adding compensatory  $O(\alpha \log^2 \alpha)$

and  $O(\alpha \log^2 \alpha)$  terms on the right-hand side to ensure that asymptotic equivalence to order  $\alpha$  is maintained. We can further replace each occurrence of  $\sigma_0 - \sigma$  above by  $\sigma_0 - \sigma - \alpha \log^2 \alpha / 2 - \mu \alpha \log \alpha$  without disturbing this equivalence, to get

$$\begin{aligned}
 P \sim & P(t_c) - \frac{1}{\gamma - 1} \log(1 - \sigma/\sigma_0 - \alpha \log^2 \alpha / 2\sigma_0 - \mu \alpha \log \alpha / \sigma_0) \\
 & - \alpha \log^2 \alpha \frac{1}{2(\gamma - 1)(\sigma_0 - \sigma - \alpha \log^2 \alpha / 2 - \mu \alpha \log \alpha)} \\
 & - \alpha \log \alpha \frac{\mu}{(\gamma - 1)(\sigma_0 - \sigma - \alpha \log^2 \alpha / 2 - \mu \alpha \log \alpha)} \\
 & + \alpha \log \alpha \frac{1 + \log(1 - \sigma/\sigma_0 - \alpha \log^2 \alpha / 2\sigma_0 - \mu \alpha \log \alpha / \sigma_0)}{(\gamma - 1)(\sigma_0 - \sigma - \alpha \log^2 \alpha / 2 - \mu \alpha \log \alpha)} \\
 & - \alpha \frac{1}{2(\gamma - 1)(\sigma_0 - \sigma - \alpha \log^2 \alpha / 2 - \mu \alpha \log \alpha)} \left[ \log^2(1 - \sigma/\sigma_0 - \alpha \log^2 \alpha / 2\sigma_0 - \mu \alpha \log \alpha / \sigma_0) \right. \\
 & \left. - \frac{2Q}{\gamma - 1} \log(1 - \sigma/\sigma_0 - \alpha \log^2 \alpha / 2\sigma_0 - \mu \alpha \log \alpha / \sigma_0) + 2 \log \pi + 2 \log(1 + \eta) \right].
 \end{aligned} \tag{7.2}$$

Here,

$$\mu = 1 + \frac{Q}{\gamma - 1}. \tag{7.3}$$

The new time variable  $\lambda$  is now defined via the transformation

$$\sigma_0 - \sigma - \frac{1}{2} \alpha \log^2 \alpha - \mu \alpha \log \alpha = \alpha \log \lambda, \tag{7.4}$$

which involves a stretching  $\alpha$  and a shift  $(1/2)\alpha \log^2 \alpha + \mu \alpha \log \alpha$ , and is equivalent to the linear scaling

$$t_c - t = e^{-\sigma/\alpha} = \exp\left(-\frac{\sigma_0}{\alpha} + \frac{1}{2} \log^2 \alpha + \mu \log \alpha\right) \lambda \equiv \delta \lambda, \tag{7.5}$$

where  $\delta$  as defined above is the linear stretching for the transition region. Then, following some algebraic manipulation, (7.2) assumes the form

$$\begin{aligned}
 P \sim & -\frac{1}{\gamma - 1} \log \alpha + P(t_c) - \frac{1}{\gamma - 1} \log \frac{\log \lambda}{\sigma_0} \\
 & + \frac{1}{(\gamma - 1) \log \lambda} \left[ -\frac{1}{2} \log^2 \frac{\log \lambda}{\sigma_0} + \frac{Q}{\gamma - 1} \log \frac{\log \lambda}{\sigma_0} - \log \pi - \log(1 + \eta) \right].
 \end{aligned} \tag{7.6}$$

This expression provides, as  $\lambda \rightarrow \infty$ , the matching condition for  $P$  in the transition region. A similar consideration of (6.81) and (6.83) leads to the corresponding conditions for  $\mathcal{T}$  and  $U$ ,

$$\mathcal{T} \sim \frac{\sigma_0}{\alpha} - \frac{1}{2} \log^2 \alpha - \mu \log \alpha - \log \lambda - \log\{1 + (\gamma - 1)\eta \log \lambda\}, \tag{7.7}$$

$$U \sim \frac{1}{\alpha(\gamma - 1) \log \lambda} [\log\{1 + (\gamma - 1)\eta \log \lambda\} - \log(1 + \eta)]. \tag{7.8}$$

The transition region sits atop the hot spot, and in it the spatial coordinate  $z$  is taken to be

$$z = \frac{\alpha x}{\delta}, \quad \text{or equivalently,} \quad z = \lambda \eta. \quad (7.9)$$

Then the induction equations (3.6)–(3.8) transform into

$$-\alpha \frac{\partial U}{\partial \mathfrak{t}} + \frac{\partial P}{\partial z} = 0, \quad (7.10)$$

$$-\frac{\partial P}{\partial \lambda} + \frac{\partial U}{\partial z} = \exp\left(-\frac{\sigma_0}{\alpha} + \frac{1}{2} \log^2 \alpha + \mu \log \alpha + \mathcal{T}\right), \quad (7.11)$$

$$-\frac{\partial \mathcal{T}}{\partial \lambda} + (\gamma - 1) \frac{\partial P}{\partial \lambda} = \exp\left(-\frac{\sigma_0}{\alpha} + \frac{1}{2} \log^2 \alpha + \mu \log \alpha + \mathcal{T}\right). \quad (7.12)$$

Guided by the matching conditions (7.6)–(7.8) we seek the transition solution in the form

$$\mathcal{T} \sim \frac{\sigma_0}{\alpha} - \frac{1}{2} \log^2 \alpha - \mu \log \alpha + \check{\mathcal{T}}, \quad (7.13)$$

$$P \sim -\frac{1}{\gamma - 1} \log \alpha + \check{P}, \quad (7.14)$$

$$U \sim \frac{1}{\alpha} \check{U}. \quad (7.15)$$

Then (7.10)–(7.12) become

$$-\frac{\partial \check{U}}{\partial \lambda} + \frac{\partial \check{P}}{\partial z} = 0, \quad (7.16)$$

$$-\frac{\partial \check{P}}{\partial \lambda} + \frac{\partial \check{U}}{\partial z} = e^{\check{\mathcal{T}}}, \quad (7.17)$$

$$-\frac{\partial \check{\mathcal{T}}}{\partial \lambda} + (\gamma - 1) \frac{\partial \check{P}}{\partial \lambda} = e^{\check{\mathcal{T}}}. \quad (7.18)$$

These are the full Clarke equations, valid in the domain  $z > 0$ ,  $\lambda < \infty$ . The absence of  $\alpha$  multiplying the acceleration term in the momentum equation indicates that pressure gradients are no longer negligible, and that the balance is now fully acoustic-reactive. Initial conditions for these equations come from the matching requirements (7.6)–(7.8), and the boundary condition is  $\check{U}(0, \lambda) = 0$ . While the solution is only obtainable numerically, its behavior is well-known [7]. In particular,  $\check{\mathcal{T}}$  and  $\check{P}$  display, at the hot wall  $z = 0$ , similar logarithmic singularities,

$$\check{\mathcal{T}} \sim -\log(\lambda - \lambda_c) + O(1),$$

$$\gamma \check{P} \sim -\log(\lambda - \lambda_c) + O(1),$$

as  $\lambda \rightarrow \lambda_c$ , a numerically determined blowup time. Correspondingly, the specific-volume perturbation  $\check{V} = \check{\mathcal{T}} - \gamma \check{P}$  remains bounded. Thus the blowup is at nearly constant volume, or inertially confined. The singularity structure of the blowup, as well as its connection with the post-induction explosive phase, are also described in detail in [7].

## 8. Closing Comments

We have investigated the singularity structure of the small-disturbance induction equations for a narrow domain of length  $\alpha$  relative to the acoustic length at the initial induction time. This work complements an earlier study [7], in which the corresponding problem was studied for  $\alpha$  of order unity. In that case the singularity was of the nearly-constant-volume variety, *i.e.*, once the hot spot began to grow in earnest the material within it remained inertially confined. Here the runaway begins with a nearly-constant-pressure character. As the hot spot grows in strength, it shrinks in size and its evolution is described by means of a small- $\alpha$  asymptotic treatment. The analysis requires consideration of a number of spatio-temporal regions, culminating in an exponentially thin domain in which the full induction (Clarke) equations, corresponding to  $\alpha = 1$ , are reinstated, *i.e.*, the hitherto spatially uniform pressure rise is replaced by circumstances in which significant pressure gradients appear. Further evolution within this thin domain would occur as if  $\alpha$  were unity. This work is yet another illustration of the versatility and ubiquity of the Clarke equations which tend to appear, if not at the outset, then at a later stage of evolution in a variety of configurations including, for example, ignition in a pulse steepening in a reactive atmosphere [12].

## Acknowledgements

Partial support for this work was provided by the Los Alamos National Laboratory, the Air Force Office of Scientific Research and the National Science Foundation.

## Appendix

### A1. DETAILS OF THE INITIAL LAYER IN THE INDUCTION DOMAIN

With

$$t = \alpha\theta, \quad P = \alpha\mathcal{P}, \quad \mathcal{T} = -\log(1 + ax) + \alpha\Phi, \quad U = \mathcal{U},$$

the induction equations (3.6)–(3.8) take the following form in the initial layer:

$$\mathcal{U}_\theta + \mathcal{P}_x = 0, \quad \mathcal{U}_x + \mathcal{P}_\theta = e^{-\log(1+ax)+\alpha\Phi}, \quad \Phi_\theta - \alpha(\gamma - 1)\mathcal{P}_\theta = e^{-\log(1+ax)+\alpha\Phi}. \quad (\text{A1})$$

The initial conditions are

$$\mathcal{P}(x, 0) = 0, \quad \mathcal{U}(x, 0) = U_i(x), \quad \Phi(x, 0) = 0, \quad (\text{A2})$$

and boundary conditions

$$\mathcal{U}(0, \theta) = \mathcal{U}(1, \theta) = 0. \quad (\text{A3})$$

We expand the solution as

$$\mathcal{P} \sim \mathcal{P}_0 + \alpha\mathcal{P}_1, \quad \mathcal{U} \sim \mathcal{U}_0 + \alpha\mathcal{U}_1, \quad \Phi \sim \Phi_0 + \alpha\Phi_1. \quad (\text{A4})$$

The leading terms satisfy

$$\mathcal{U}_{0\theta} + \mathcal{P}_{0x} = 0, \quad \mathcal{U}_{0x} + \mathcal{P}_{0\theta} = \frac{1}{1 + ax}, \quad \Phi_{0\theta} = \frac{1}{1 + ax}.$$

The last of these, subject to the null initial condition, yields the integral

$$\Phi_0 = \frac{\theta}{1 + ax}, \quad (\text{A5})$$

thereby allowing the first two to integrate to

$$\mathcal{U}_0 + \mathcal{P}_0 = \frac{1}{a} \log(1 + ax) + f_0(\theta - x), \quad (\text{A6})$$

$$\mathcal{U}_0 - \mathcal{P}_0 = \frac{1}{a} \log(1 + ax) + g_0(\theta + x). \quad (\text{A7})$$

Application of the initial and boundary data followed by some algebraic manipulation leads to the determination of  $f_0$  and  $g_0$ , and we obtain

$$g_0(\theta) = -f_0(\theta), \quad \theta > 0, \quad (\text{A8})$$

$$f_0(\theta) = \frac{\theta}{a} \log(1 + a) + \mathcal{G}_0(\theta), \quad \theta > -1. \quad (\text{A9})$$

Here  $\mathcal{G}_0(\theta)$  is the periodic extension, with period 2, of the odd function  $G_0(\theta)$  given by

$$G_0(\theta) = \begin{cases} -\frac{1}{a} \log(1 - a\theta) - \frac{\theta}{a} \log(1 + a) + U_i(-\theta), & \text{for } -1 < \theta < 0, \\ \frac{1}{a} \log(1 + a\theta) - \frac{\theta}{a} \log(1 + a) - U_i(\theta), & \text{for } 0 < \theta < 1. \end{cases} \quad (\text{A10})$$

With  $f_0(s)$  determined, we return to (A6) and (A7) to obtain

$$\mathcal{U}_0 = \frac{1}{a} \log(1 + ax) - \frac{x}{a} \log(1 + a) + \frac{1}{2} [\mathcal{G}_0(s - x) - \mathcal{G}_0(s + x)], \quad (\text{A11})$$

$$\mathcal{P}_0 = \frac{\theta}{a} \log(1 + a) + \frac{1}{2} [\mathcal{G}_0(s - x) + \mathcal{G}_0(s + x)]. \quad (\text{A12})$$

Let us examine the behavior of this solution for  $\theta$  large, by setting  $\theta = t/\alpha$ .

$$\begin{aligned} U &\sim \mathcal{U}_0 \\ &\sim \frac{1}{a} \log(1 + ax) - \frac{x}{a} \log(1 + a) + \frac{1}{2} \left[ \mathcal{G}_0\left(\frac{t}{\alpha} - x\right) - \mathcal{G}_0\left(\frac{t}{\alpha} + x\right) \right], \end{aligned} \quad (\text{A13})$$

$$\begin{aligned} P &\sim \alpha \mathcal{P}_0 \\ &\sim \frac{t}{a} \log(1 + a) + \frac{\alpha}{2} \left[ \mathcal{G}_0\left(\frac{t}{\alpha} - x\right) + \mathcal{G}_0\left(\frac{t}{\alpha} + x\right) \right]. \end{aligned} \quad (\text{A14})$$

These expressions provide matching conditions for the solution in the main induction region. They imply that in that region the pressure consists of an order-unity portion that is independent of  $x$  and varies only with  $t$ , and an order  $\alpha$  portion that varies on the rapid time scale  $t/\alpha$  but only (slowly) on the spatial coordinate  $x$ . Similarly the velocity also has a slow and a fast component, but now both order-unity in amplitude. The fast components do not match with the solution in the main induction region, as developed in Section 3 in the text.

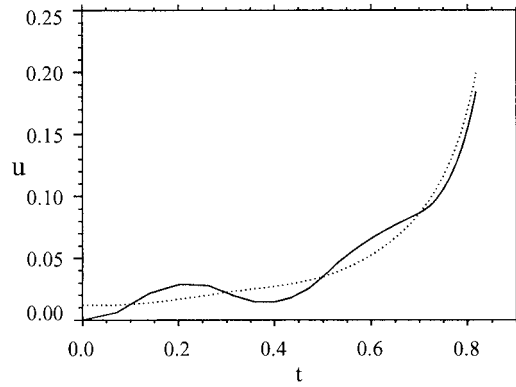


Figure A.1. Graphs of the numerically-computed mid-slot velocity  $U(0.5, t)$  in the induction stage. The full-line curve corresponds to zero initial velocity and the dotted-line curve to the special initial velocity  $U(x, 0)$  given by equation (A15) below. The appearance of oscillations for the former condition is clearly evident.

The reason, of course, is that in the main induction region, we have effectively disallowed, or filtered out, the fast components by selecting  $t$  as the only time scale. This filtering can be switched off by allowing the outer solution to vary on both the slow and fast time scales. We can eliminate the fast components (and hence the need for an initial layer) altogether by a proper choice of a (nonzero) initial condition for  $\mathcal{U}$ . Such a condition, corresponding to  $\mathcal{G}_0 \equiv 0$ , is clearly seen from (A10) to be

$$U_i(x) = \frac{1}{a} \log(1 + ax) - \frac{x}{a} \log(1 + a), \tag{A15}$$

and is the one employed in the analysis in Section 3.

Figure A.1 above displays the numerically-computed time-evolution of  $U$  in the induction stage at the mid point of the domain for two initial conditions. High-frequency oscillations appear in the profile for null initial condition, but are suppressed for the special choice  $U_i(x)$ .

A2. ASYMPTOTIC BEHAVIOR OF  $f_1(\tau)$  AND  $g_1(\tau)$  AS  $\tau \rightarrow 0$

We recall from (4.25) that  $f_1(\tau)$  is defined by

$$f_1(\tau) = \frac{c}{2a} \log(2\pi) - \frac{c(\tau + 1)}{2a} \log \frac{2c}{a} - \frac{c}{a} \log \left[ \gamma \left( 1 + \frac{\tau}{2} \right) \right]. \tag{A16}$$

Now it is known (Abramowitz and Stegun [13, p. 256]) that

$$\frac{1}{\Gamma(1 + z)} = \frac{1}{z\Gamma(z)} \sim 1 + \gamma_0 z + O(z^2) \text{ as } z \rightarrow 0,$$

where  $\gamma_0$  is Euler's constant. Then

$$\log \Gamma(1 + z) = -\log\{1 + \gamma_0 z + O(z^2)\} \sim -\gamma_0 z + O(z^2) \text{ as } z \rightarrow 0.$$

Upon substitution of this result in (A16) we get

$$f_1(\tau) \sim \frac{c}{2a} \log \frac{\pi a}{c} + \frac{c\tau}{2a} \left( \gamma_0 - \log \frac{2c}{a} \right) + O(\tau^2) \text{ as } \tau \rightarrow 0. \tag{A17}$$

Now recall from (4.19) that  $g_1(\tau)$  is given by

$$g_1(\tau) = -\frac{c}{a} \log \frac{c\tau}{a} - f_1(\tau), \quad (\text{A18})$$

so that the use of (A17) leads to

$$g_1(\tau) \sim -\frac{c}{a} \log \frac{c\tau}{a} - \frac{c}{2a} \log \frac{\pi a}{c} - \frac{c\tau}{2a} \left( \gamma_0 - \log \frac{2c}{a} \right) + O(\tau^2) \text{ as } \tau \rightarrow 0. \quad (\text{A19})$$

Finally, (A17) and (A19) combine to yield

$$-f_1(\tau) + g_1(\tau) \sim -\frac{c}{a} \log(\pi\tau) - \frac{c\tau}{a} \left( \gamma_0 - \log \frac{2c}{a} \right) + O(\tau^2) \text{ as } \tau \rightarrow 0. \quad (\text{A20})$$

## References

1. D.R. Kassoy, A.K. Kapila and D.S. Stewart, A unified formulation for diffusive and nondiffusive thermal explosion theory. *Combust. Sci. Tech.* 63 (1989) 33–43.
2. J.F. Clarke, Finite amplitude waves in combustible gases, In: J.D. Buckmaster (ed.), *The Mathematics of Combustion*. Philadelphia: SIAM Publications (1985) pp. 183–246.
3. J.F. Clarke and R.S. Cant, Unsteady gasdynamic effects in the induction domain behind a strong shock wave. *Prog. Astron. Aeron.* 95 (1984) 142–163.
4. T.L. Jackson and A.K. Kapila, Shock-induced thermal runaway. *SIAM J. Appl. Math.* 45 (1985) 130–137.
5. J.W. Dold, A.K. Kapila and M. Short, Theoretical description of direct initiation of detonation for one-step chemistry, In: A.A. Borisov (ed.), *Dynamic Structure of Detonation in Gaseous and Dispersed Media*. Dordrecht: Kluwer Academic Publishers (1991) pp. 109–141.
6. A.K. Kapila, D. W. Schwendeman, J. J. Quirk and T. Hawa, Mechanisms of detonation formation due to a temperature gradient. *Comb. Theory Modelling* 6 (2002) 553–544.
7. T.L. Jackson, A.K. Kapila and D.S. Stewart, Evolution of a reactive center in an explosive material. *SIAM J. Appl. Math.* 49 (1989) 432–458.
8. C.J. Parkins, P.A. Blythe and D.G. Crighton, Hot spot ignition: the Newtonian limit. *Proc. R. Soc. London A* 456 (2000) 2857–2882.
9. P.A. Blythe and D.G. Crighton, Shock-generated ignition: the induction zone. *Proc. R. Soc. London A* 426 (1989) 189–209.
10. C.J. Parkins, Shock-generated ignition, Newtonian asymptotics for the induction domain between a contact surface and shock. *SIAM J. Appl. Math.* 61 (2000) 701–729.
11. D.R. Kassoy, N. Riley, J. Beberness and A. Bressan, The confined nondiffusive thermal explosion with spatially homogeneous pressure variation. *Combust. Sci. and Tech.* 63 (1989) 45–62.
12. J.J. Quirk, T.L. Jackson and A.K. Kapila, Evolution of a compressive pulse in a reactive atmosphere: transition to detonation, In: M.Y. Hussaini, T.B. Gatski and T.L. Jackson (eds.), *Transition, Turbulence and Combustion, Vol II*. Dordrecht: Kluwer Academic Publishers (1994) pp. 313–329.
13. M. Abramowitz and I. A. Stegun, *Handbook of Mathematical Functions*. Washington: National Bureau of Standards (1964) 1046 pp.